A Comparison of Large and Small Tropical Cyclones

by
Robert Travis Merrill

P.I. William M. Gray

Department of Atmospheric Science
Colorado State University
Fort Collins, Colorado

NOAA NA8IRAD00005
NOAA NA8IRH00001
NSF ATM-7923591

Colorado State University

Department of Atmospheric Science

Paper No. 352

A COMPARISON OF LARGE AND SMALL TROPICAL CYCLONES

By

Robert Travis Merrill

Department of Atmospheric Science

Colorado State University

Fort Collins, Colorado

July, 1982

Atmospheric Science Paper No. 352

ABSTRACT

The structure of the wind field of a tropical cyclone can be roughly described by three measurements: intensity (maximum wind), size (extent of the vortex), and strength (average wind speed of the vortex). This paper examines the climatology, structure and possible physical processes of tropical cyclones of different sizes. Records of tropical cyclone sizes, as indicated by the radius of the outer closed isobar (ROCI) are described for the period 1961-1969 in the western North Pacific and 1957-1977 in the Atlantic. The climatology of cyclone sizes confirms that typhoons are characteristically twice as large as hurricanes, and also reveals that the typical size of cyclones varies seasonally and regionally within ocean basins and is only weakly correlated with cyclone intensity (maximum wind or minimum pressure). Rawinsonde composites of large and small tropical cyclones show that large cyclones have much more relative angular momentum (RAM) than small ones, while the differences in RAM between intense and weaker cyclones of equivalent size are much less. Some of the implications of this observation are discussed, and a hypothesis that cyclones grow as a result of an increased convergence of angular momentum forced by their environment is presented.

TABLE OF CONTENTS

1. INTRODUCTION

Tropical cyclones have been the subject of extensive study for many years - forecasters have charted their tracks and described their behavior in detail, and scientists have compiled observations of these storms and performed numerical experiments in an effort to unlock their physics. These efforts have met with limited success - we know more about tropical cyclones than we did 25 years ago, but some aspects of tropical cyclone meteorology have gone nearly untouched. In particular, the structure of the hurricane vortex, in terms of its intensity, strength and size, has yet to be fully described.

The term 'tropical cyclone' implies a neat classification. Yet within this classification we find storms as diverse as cyclone 'Tracy', which struck Darwin, Australia in 1974, and Supertyphoon 'Tip', which occurred in the northwest Pacific in 1979. Tracy had gale force winds (17 m s^{-1}) over an area only 100 km across, though its peak winds of 65 m s^{-1} made it a severe hurricane (Australian Bureau of Meteorology, 1977). Tip, on the other hand, spread gale force winds over a 2200 km diameter, an area hundreds of times larger than Tracy (Dunnavan and Diercks, 1980). Figure 1 shows two examples from the Atlantic basin. Camille had maximum winds of 85 m s^{-1}, while Faith, though much larger, had only 50 m s^{-1} winds. Even within a single season, tropical cyclones come in all sizes just as they move in a variety of ways and attain a variety of intensities.

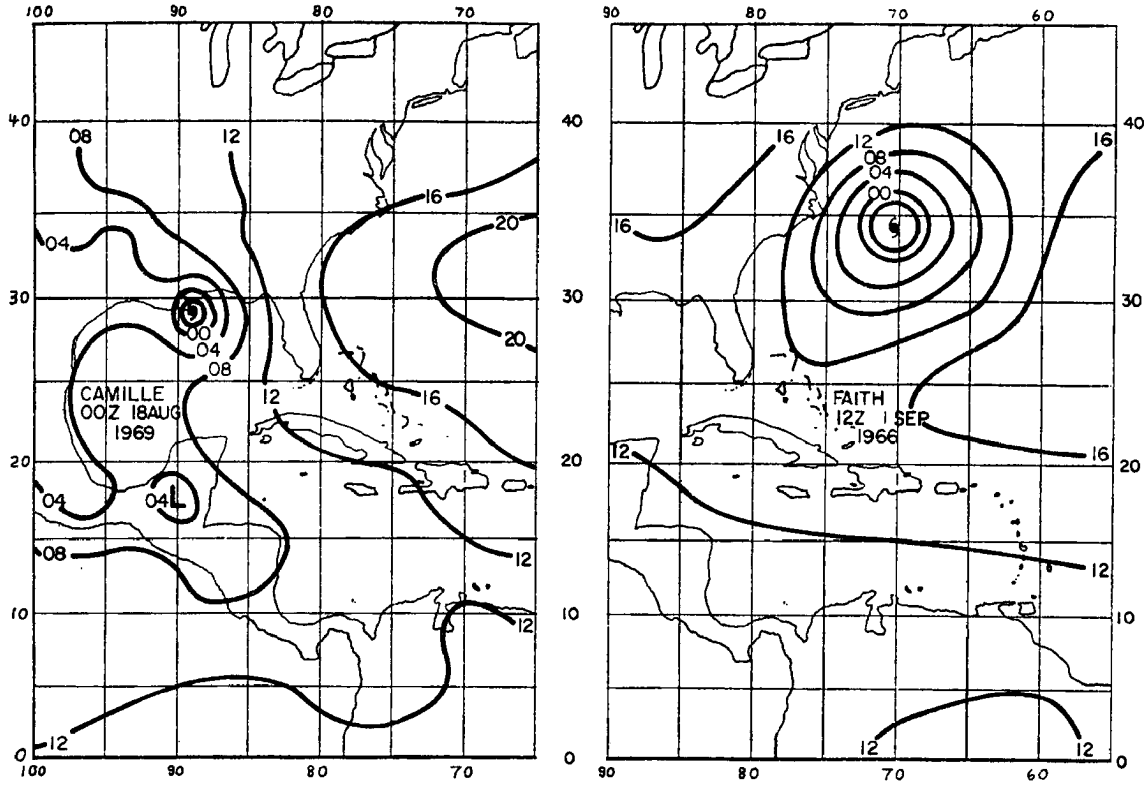

Fig. 1. Surface pressure analyses for Camille, a small, intense hurricane (left) and Faith, a larger but weaker one (right).

The issue of cyclone size is not unimportant, either. A small, intense hurricane or typhoon is easily avoided by shipping, while a larger, yet weaker one, can produce heavy seas over a large area and greatly hamper sea traffic. Other practical concerns come to mind: do large hurricanes break up over land less rapidly, carrying damaging winds inland far enough to reach populated areas which would otherwise go untouched? Will a large cyclone produce more tornadoes or torrential rains than a smaller one? One of the purposes of the research being presented in this paper is to make these and other investigations possible at a later date by building a data set and climatology of cyclone size. These are described in Chapters 2 and 3 respectively.

Equally important are the implications cyclone size has on cyclone dynamics. Large cyclones spread relatively high winds over a larger area and are thus exposed to greater surface losses of angular momentum and kinetic energy, but also gain more moisture through evaporation. The physical influences these processes have on the intensity of the cyclone are not known - nor is it clear how large and small cyclones might interact with their environment. Chapter 4 describes the structure of large and small cyclones and Chapter 5 discusses how these structural differences might affect the dynamics of the cyclone.

1.1 Definitions

The topic of cyclone size is a relatively new one, and some confusion has arisen in the past over the terms 'size', 'strength', 'intensity', 'growth', etc. A major point of this paper is that changes in the structure of a tropical cyclone vortex can occur in several different modes. These modes are illustrated in Fig. 2 and described below. A summary is given in Table 1.

Intensity. A measure of the extreme value of a meteorological variable in a tropical cyclone. Minimum sea level pressure (MSLP) and maximum sustained winds are usually used to describe the intensity of a cyclone. Intensification refers to a decrease in MSLP or an increase in maximum winds.

Size. The areal extent of a tropical cyclone circulation. It is operationally measured as the extent of winds above a certain speed, usually gale force (17 m s^{-1}), or as the average radius of outer closed isobar (ROCI). The latter is used throughout this paper. Growth refers to an expansion of the tropical cyclone circulation.

Strength. The average wind speed in the cyclone circulation. Note from Fig. 2 that the strength of a cyclone can change even though the intensity (maximum wind) and size (extent of gales) remain constant. Strength is not dealt with explicitly in this paper.

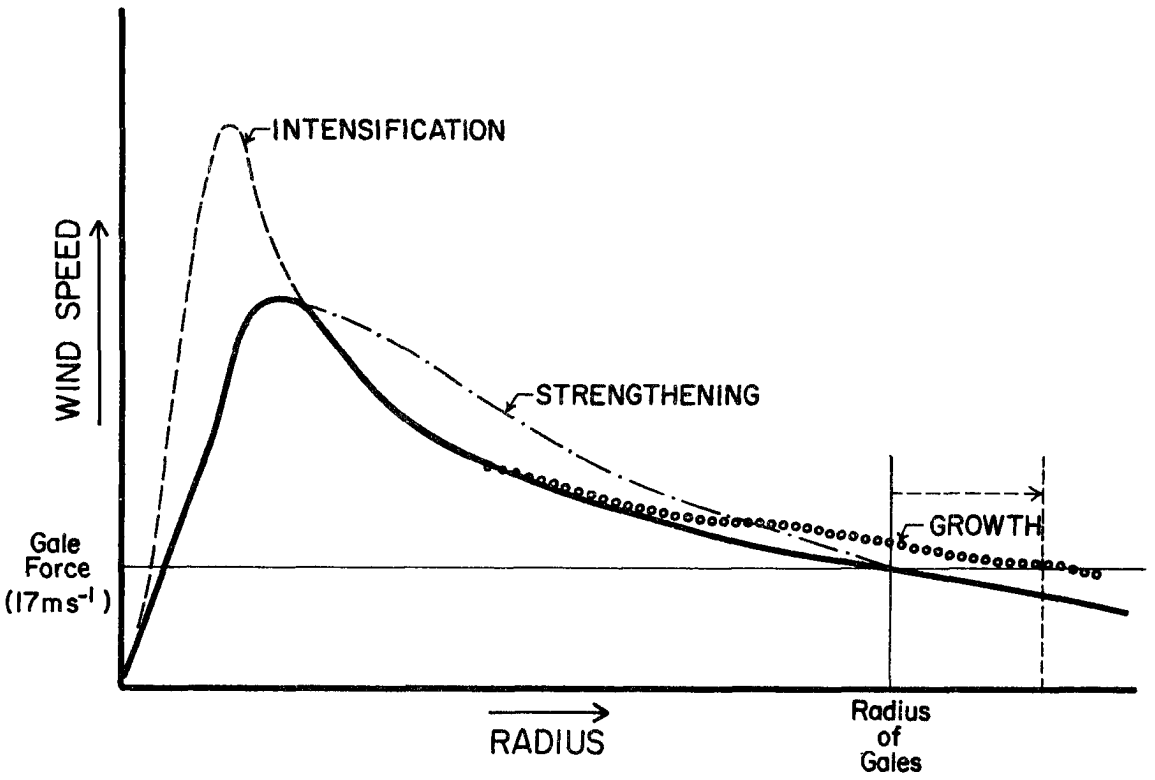

Fig. 2. Schematic of the changes in lower tropospheric tangential wind associated with intensification, strengthening, and growth of a tropical cyclone.

TABLE 1

Definitions of the structure of the tropical cyclone wind field.

Description	Definition	Increase with Time
Intensity	Maximum wind or Minimum Sea Level Pressure	Intensification
Strength	Average Wind Speed Within the Circulation	Strengthening
Size	Extent of the Cyclone Circulation (radius of Gales or of Outer Closed Isobar)	Growth

2. DESCRIPTION OF DATA

Four data sets are used in this paper: 1) A set of cyclone positions and sizes for the Atlantic basin, 1957-1977, 2) positions and sizes for the western North Pacific basin, 1961-1969, 3) Atlantic basin rawinsonde observations (Fig. 3) for 1957-1977, and 4) Pacific rawinsonde observations (Fig. 4) for 1961-1969. The tropical cyclone size climatology presented in Chapter 3 is based on the position and size records, and the structure of large and small cyclones as described in Chapter 4 is determined by compositing the rawinsonde observations. The rawinsonde data sets and the compositing approach have been in existence for several years and have been widely used by other members of Professor Gray's tropical cyclone research project. The size records are much less well documented, and did not even exist for the Atlantic prior to this study. Both the rawinsonde data and the track/size data are described in greater detail below.

2.1 Rawinsonde Data

Two rawinsonde data sets were used to examine the structure of large and small cyclones - an Atlantic set consisting of about 50,000 soundings from 103 stations over a period of 21 years from 1957-1977, and a Pacific set, with about 18,000 soundings from 28 stations over a 9 year period from 1961-1969. The location of the rawinsonde stations for the Atlantic and Pacific sets are shown in Figs. 3 and 4 respectively. The Pacific set is a subgroup of the 10 year (1961-1970) rawinsonde set used by Frank (1977) and George and Gray (1977) in studies of typhoon

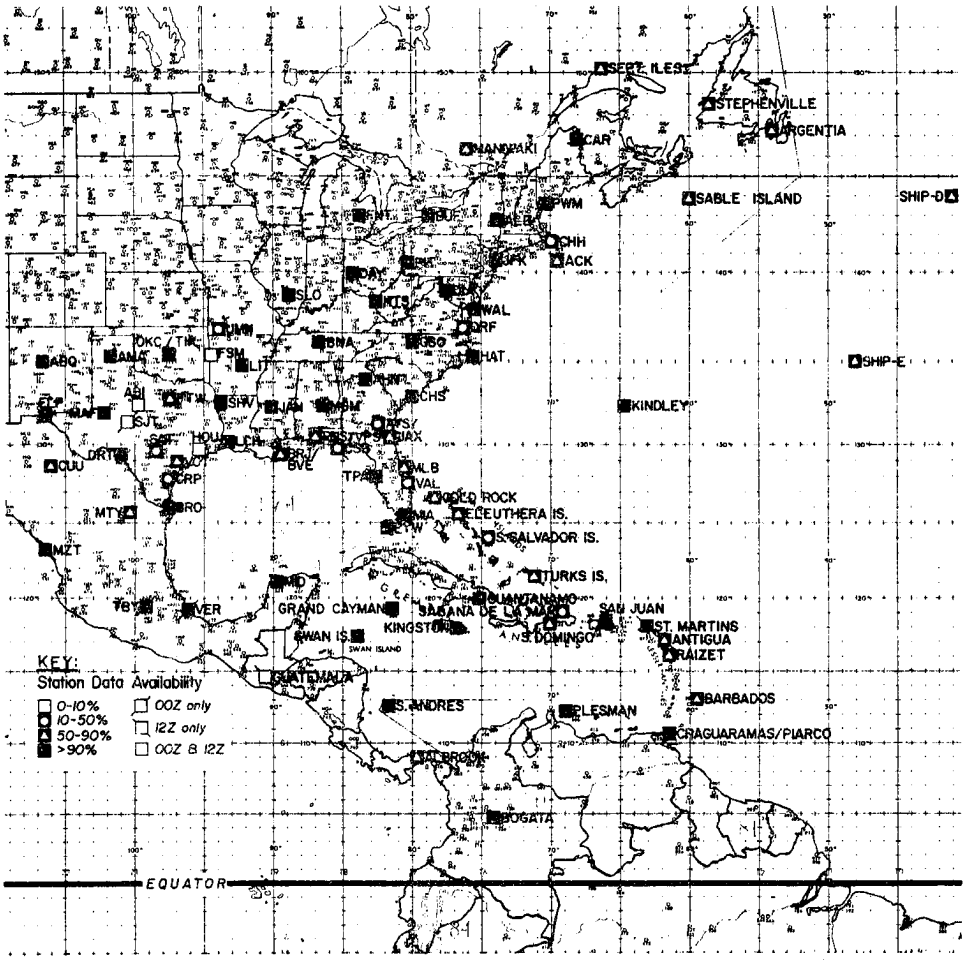

Fig. 3. Location of Atlantic rawinsonde observations making up the rawinsonde composites.

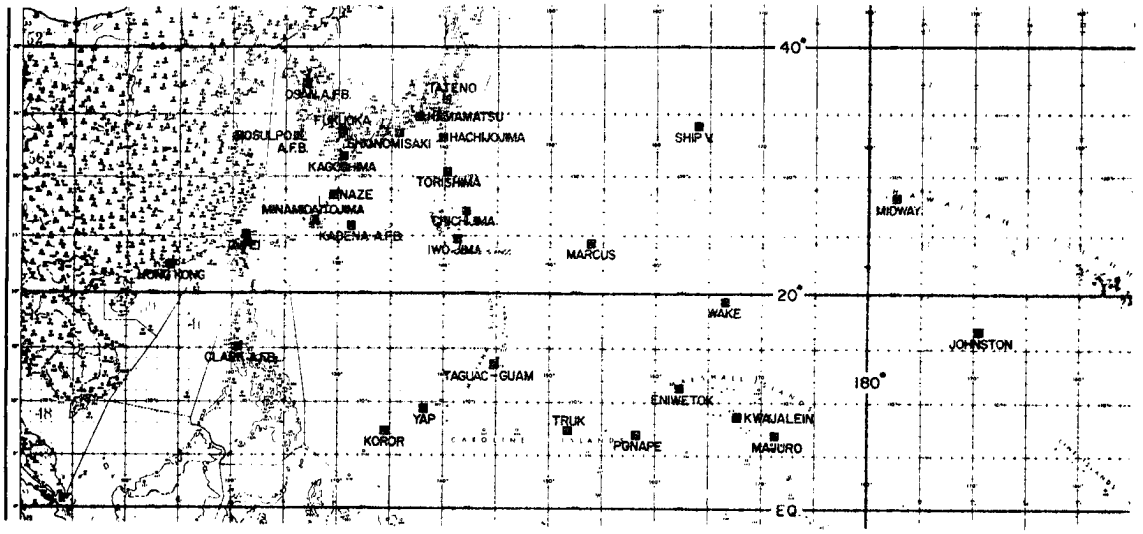

Fig. 4. Location of Pacific rawinsonde observations making up the rawinsonde composites.

structure, energetics and motion. The Atlantic set is an extension of the 14 year (1961-1974) set used in structure and motion studies of Atlantic tropical weather systems by Chan et al. (1980), Frank and Gray (1980) and McBride and Zehr (1981). The contents of these sets, the details of their preparation, and the rawinsonde compositing method are described in Gray et al. (1982).

2.2 Tropical Cyclone Position and Size Records

The Pacific cyclone position and size data were prepared at the Joint Typhoon Warning Center on Guam and made available by the Naval Environmental Prediction Research Facility (NEPRF) at Monterey, CA. Each record consists of a position, maximum wind, minimum sea level pressure (MSLP), speed and direction of motion, and average radius of outer closed isobar (ROCI) at 00 GMT and 12 GMT for tropical storms and typhoons during 1961-1969. The set includes 201 cyclones and a total of 2576 records.

The Atlantic basin position set was built using the National Hurricane Center (NHC) track file (Jarvinen and Caso, 1978) which consists of position, estimated maximum sustained winds, and MSLP (where available) at 6 hour intervals. These records were used to compute speed and direction at 00 GMT and 12 GMT, and then merged with ROCI data (determined as described below) to obtain complete records, analogous to those for the Pacific, for the tropical storms and hurricanes of 1957-1977. The Atlantic position set contains 183 cyclones and 1722 position records.

Measurements of the radius of outer closed isobar are not recorded operationally in the Atlantic, and therefore had to be extracted from archived NHC surface analyses, available on microfilm at Colorado State

University. The ROCI is defined as the average of the distances to the north, east, south and west of the cyclone center to the closed isobar having the highest value. These values are expressed in whole degrees latitude so as to be compatible with existing data for Pacific cyclones. Prior to 1964, charts were analyzed at 3 mb intervals and had to be redrawn at 2 mb intervals for consistency with Pacific and later Atlantic analyses, and some additional reanalysis of charts was performed when needed. Occasionally, particularly when a cyclone was just forming, the outer closed isobar was elongated or distorted. In such cases, the next-lower valued isobar was taken as the outer closed isobar. A schematic of the measurement technique is shown in Fig. 5.

The ROCI has its disadvantages as a measure of cyclone size. It is somewhat dependent on the environmental pressure gradient, is not as physically relevant as is the wind field, and is subjectively determined. It is nevertheless the best measure of cyclone size that is available throughout the life of a cyclone. Because the surface pressure is generally smooth and well-behaved, it is an easier field to estimate than is wind, which may vary sharply in the horizontal. Since a size estimate is needed for every cyclone position on file so that a climatology can be made, the ROCI is believed to be the best choice of a size estimate. In addition, the relationship between radius of outer closed isobar and the cyclone wind field is consistent and statistically sound. Evidence of this will be provided in Chapter 4.

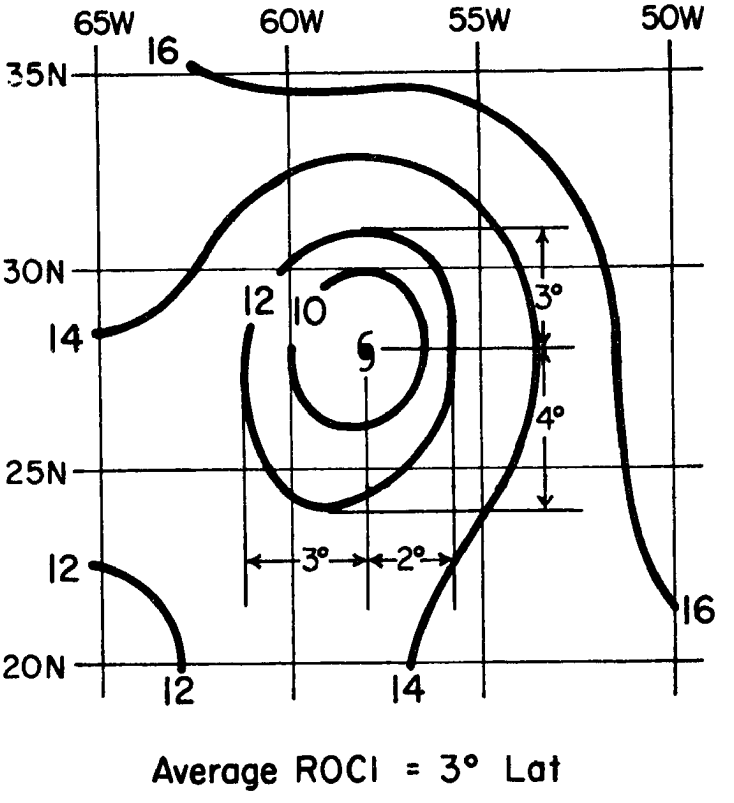

Fig. 5. Example of the method used to determine the average radius of outer closed isobar (ROCI) of a tropical cyclone.

3. CLIMATOLOGY OF TROPICAL CYCLONE SIZE

A meteorological phenomenon can often be partly understood simply by identifying where, when and with what frequency it occurs. A major component of this paper is a climatology of the tropical cyclone based on size. Such studies are few and limited in scope in the Pacific (Brand, 1972, and Arakawa, 1950) and altogether nonexistent in the Atlantic. The climatology will be developed in parallel for each basin. Four topics will be discussed in turn: 1) the overall distribution of cyclone sizes in each ocean basin, 2) the monthly variation of the size distribution, 3) the spatial variation in cyclone size across the basin, and 4) the typical changes in size during the life cycle of a typhoon or hurricane.

3.1 Overall Size Distributions

The distributions of size of all cyclones for the Atlantic (1957-1977) and Pacific (1961-1969) are shown in Figs. 6 and 7 respectively. The size difference between Atlantic and Pacific cyclones which has been previously described qualitatively (Atkinson, 1971) is plainly evident. Table 2 shows some of the statistical attributes of these distributions.

It can be seen that the ROCI of the 'mean' Pacific cyclone is about 1.5 degrees larger than that of the Atlantic cyclone. This represents a difference of about 40 percent in the mean radius between the two basins. For a circular outer closed isobar, the enclosed area is over twice as great for the Pacific cyclone.

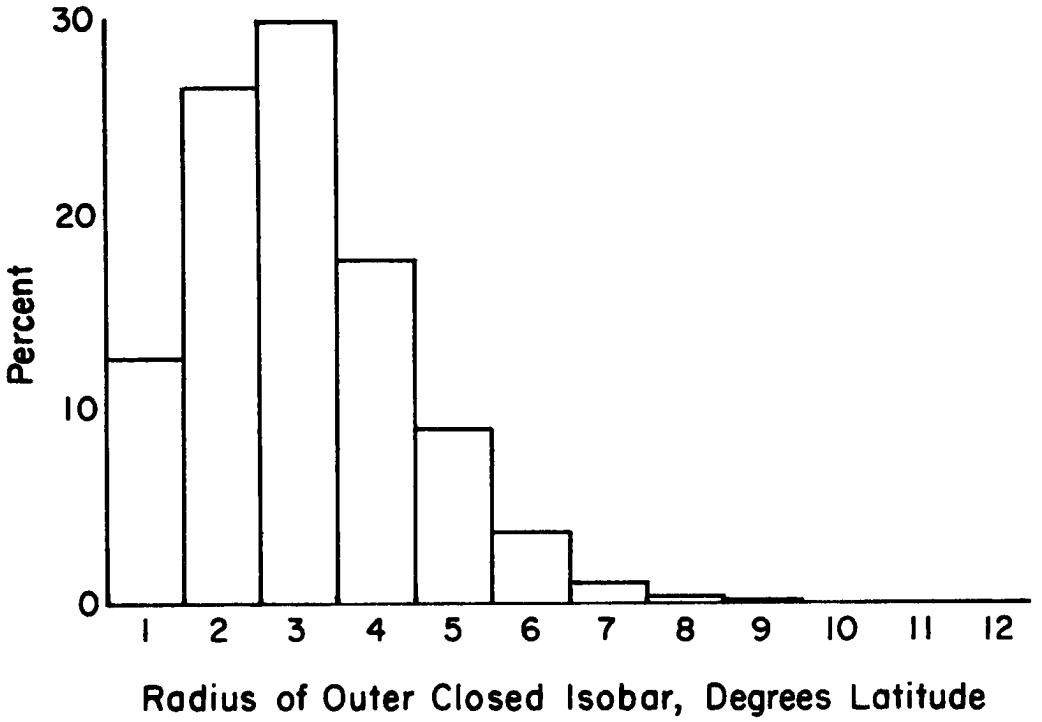

Fig. 6. Percent frequency distribution of sizes of Atlantic tropical cyclones, 1957-1977.

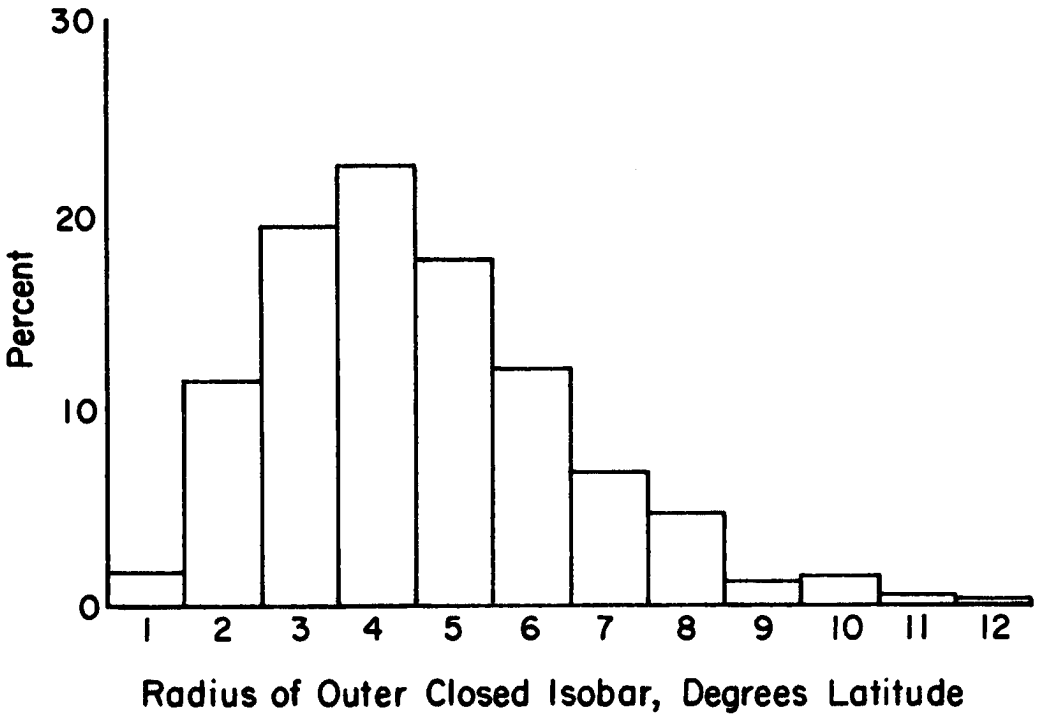

Fig. 7. Same as Fig. 6 but for the Pacific tropical cyclones, 1961-1969.

TABLE 2

Statistical attributes of the distributions of tropical cyclone size for the north Atlantic and northwest Pacific basins.

	Atlantic	Pacific
Number of Records	1722	2576
RADIUS(degrees latitude)		
Mean	3.0	4.6
Standard Deviation	1.4	2.0
Median	2.4	3.8
25th percentile	1.5	2.6
75th percentile	3.4	5.2
AREA(degrees latitude)^2		
Mean	10.9	24.5
Standard Deviation	9.8	21.8
Median	5.9	14.4
25th percentile	2.4	7.0
75th percentile	11.5	26.1

An immediate inference is that some environmental influence modulates cyclone size and causes a characteristically larger cyclone in the Pacific. If this is the case, it might be expected that this environmental control also varies seasonally. The next section examines this possibility.

3.2 Seasonal Variability of Tropical Cyclone Size

The seasonal change of cyclone size is summarized in Fig. 8 (Atlantic) and Fig. 9 (Pacific). With the exception of the relatively few Pacific cyclones which occur in the period December–April, the two curves are similar; both display a relative size minimum in mid-summer and a maximum in October. May cyclones are quite rare in the Atlantic, so that value is not too reliable.

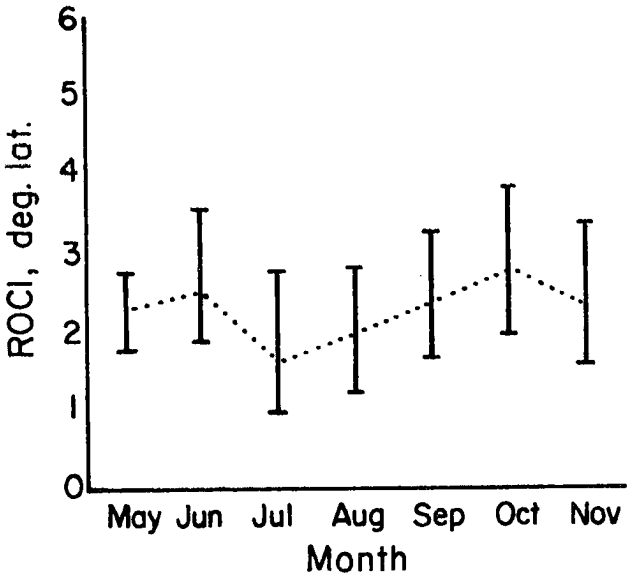

Fig. 8. Monthly progression of median, 25th, and 75th percentile of size for Atlantic tropical cyclones (includes all tropical storms and hurricanes), 1957–1977.

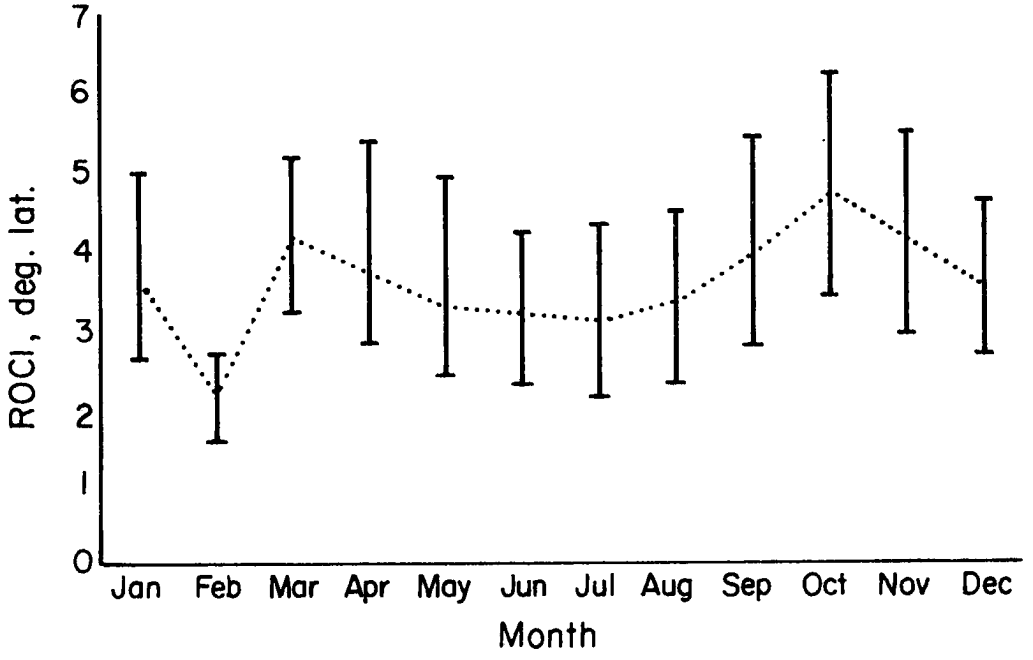

Fig. 9. Same as Fig. 8 but for the Pacific tropical cyclones (includes all tropical storms and typhoons), 1961–1969.

The simplest explanation for the seasonal variation would be to relate cyclone size and intensity, as defined by MSLP or maximum winds. The strongest cyclones would then be expected in October, with weaker ones in midsummer. Examination of the wind data show this not to be the case, however. Time series of maximum wind of tropical cyclones are presented for the Atlantic in Fig. 10 and Pacific in Fig. 11. In both basins, September cyclones are at least as intense as October ones and, although a weak intensity minimum does appear in July in the Pacific, the Atlantic shows only a monotonic increase in strength through the midsummer size minimum. Another discrepancy between intensity and size occurs in the spring in the Pacific, where the size maximum in March leads the April intensity maximum. The opposite occurs in fall in both basins; maximum intensity (September) leads maximum size (October). Although trends in intensity account for part of the seasonal trend in size, additional factors appear to be involved.

3.3 Spatial Variability of Tropical Cyclone Size

It has been shown (Dunn and Miller, 1960) that cyclone genesis occurs in different parts of the basin at different times of the year. Love (1982) has furnished evidence that periods of tropical cyclone genesis in the northwest Pacific are preceded by synoptic and planetary scale changes in the tropospheric circulation of both hemispheres. In the Atlantic, the few June cyclones that do occur usually form in the northwest Caribbean Sea and the Gulf of Mexico. The area of genesis shifts to the central tropical Atlantic in August and September and back to the Caribbean-Gulf area in October in response to environmental controls. Pacific cyclone genesis tends to follow the monsoon trough and genesis occurs at highest latitude in August (Gray, 1979 and Ding

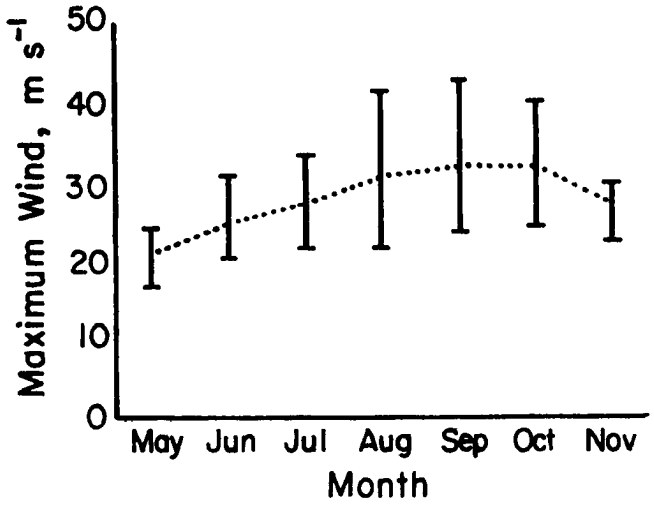

Fig. 10. Monthly progression of median, 25th, and 75th percentile values of maximum sustained wind of Atlantic tropical cyclones, 1957-1977.

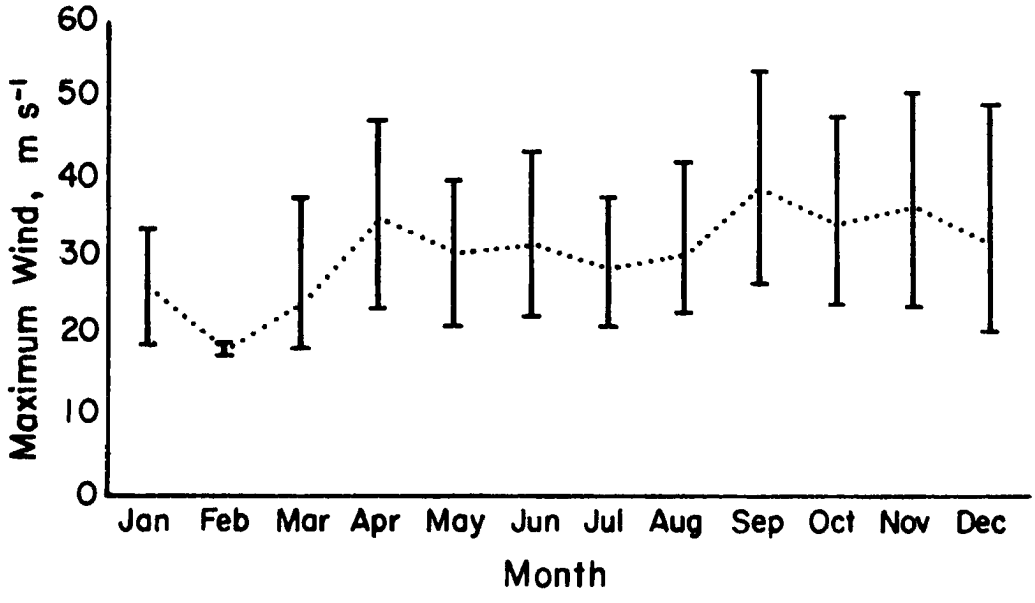

Fig. 11. Same as Fig. 10 but for the Pacific tropical cyclones, 1961-1969.

and Reiter, 1980). An examination of the size and track data for both the Atlantic and Pacific reveals similar areas where large or small cyclones typically occur; these areas also change seasonally.

To examine spatial variability, it is necessary to tabulate cyclone occurrences within relatively small regions (5 degree latitude-longitude cells are used here). When monthly tabulations are made, not enough cyclone cases are available in some areas to insure a stable mean or median. The alternative approach chosen was to divide the cyclones more coarsely into three categories: 'small', 'medium' or 'large', based on size, and subdivide each of these groups by intensity, either 'tropical storm' or 'hurricane/typhoon', for a total of 6 categories in each basin. The criteria for the categories are shown in Table 3, and the percent frequency of occurrence of each category is given in Table 4.

TABLE 3

Criteria used in classifying tropical cyclones by size and intensity in the north Atlantic and northwest Pacific.

INTENSITY	ATLANTIC	PACIFIC
Tropical Storm	Designated by National Hurricane Center, and $17 \text{ m s}^{-1} < V_{max} < 33 \text{ m s}^{-1}$	Designated by Joint Typhoon Warning Center, and MSLP > 980 mb
Hurricane/ Typhoon	$V_{max} > 33 \text{ m s}^{-1}$	Typhoon MSLP < 980 mb

V_{max} = Maximum Sustained Wind MSLP = Minimum Sea Level Pressure

SIZE		
Small	ROCI = 1-2 deg. lat.	ROCI = 1-3 deg. lat.
Medium	ROCI = 3 deg. lat.	ROCI = 4-5 deg. lat.
Large	ROCI > 3 deg. lat.	ROCI > 5 deg. lat.

ROCI = Radius of Outer Closed Isobar

TABLE 4

Frequency of occurrence of size and intensity categories as percentages of basin totals for the north Atlantic and northwest Pacific.

ATLANTIC

	Small	Medium	Large	All Sizes
Trop. Storm	23.2	11.6	9.1	43.9
Hurricane	15.6	18.4	22.1	56.1
All Intensities	38.8	30.0	31.2	100.0

PACIFIC

	Small	Medium	Large	All Sizes
Trop. Storm	24.8	19.7	8.4	52.9
Typhoon	10.5	19.6	17.0	47.1
All Intensities	35.3	39.3	25.4	100.0

The intensity criteria were chosen for consistency with the operational designation 'hurricane' in the Atlantic, and the separation for the 'typhoon' rawinsonde composite (Frank, 1977) in the Pacific. In the northwest Pacific, a pressure of 980 mb typically corresponds to a maximum wind of 30–35 m s^{-1} (Atkinson and Holliday, 1977; Dvorak, 1975) which is close to the operational separation (based on maximum wind) at 33 m s^{-1}. The size criteria were chosen so as to divide the cyclones of each basin into roughly equal thirds.

Monthly percent frequencies of these categories (the percentage of cyclones in a given month which fall into a specific category) display the same seasonal trends as the quantile time series presented in Figs. 8–11. Two examples from the Atlantic basin are shown in Figs. 12 and 13. These figures show the percentage of all tropical cyclones in a given month which are of hurricane intensity (Fig. 12) or are large

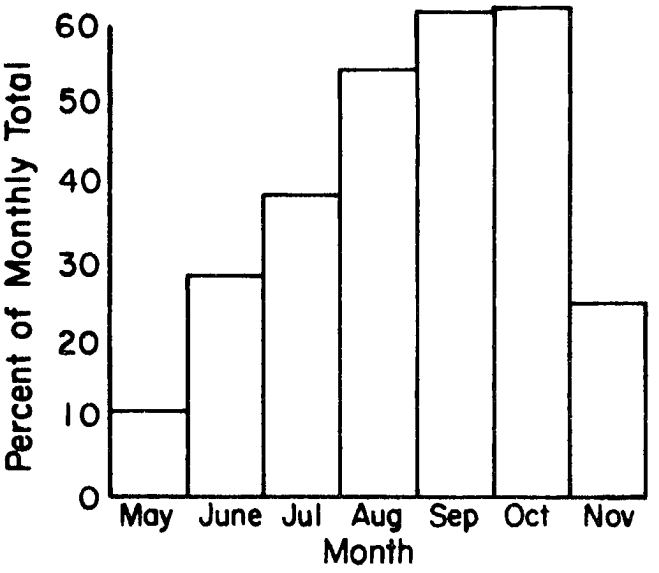

Fig. 12. Monthly percent frequencies of hurricanes for the Atlantic basin, 1957-1977.

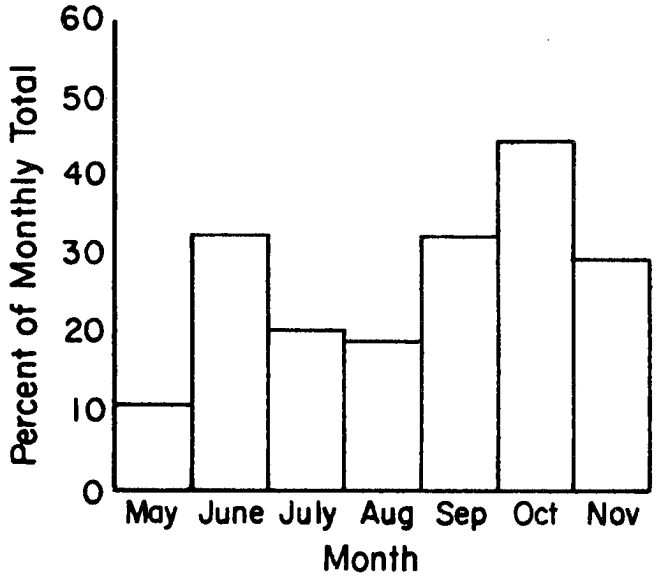

Fig. 13. Monthly percent frequencies of large tropical cyclones (hurricanes and typhoons) for the Atlantic basin, 1957-1977.

(Fig. 13). What is indicated is the percent frequency of a particular type in a given month. Note that the September–October intensity maximum and October size maximum discussed earlier are again evident. Maps of spatial relative frequencies will be used to examine geographical variability of cyclone size.

Figures 14–16 show the percent frequencies of large cyclones for the northwest Pacific for the months of August, September and October. Corresponding maps for the north Atlantic are shown in Figs. 17–19. Percent frequencies are computed for a cell only if the total number of cyclone positions is five or more. The August–October period is presented for two reasons: 1) sufficient cases are available over a large area of the basin, and 2) the period covers a transition from a month of small cyclones (August) to a month of large ones (October).

The August–October period in the Pacific will be discussed first since the two existing studies of cyclone size (Arakawa, 1950; Brand, 1972) concern this basin. The August chart in Fig. 14 shows a comparatively broken pattern, but an area of enhanced large cyclone frequency can be seen east of the Philippines, and an area of suppressed large cyclone frequency south and southwest of Japan. Brand (1972) and Arakawa (1950) have both mentioned the latter area as a region where very small typhoons tend to occur, especially in August. The size data for 1961–1969 support this observation; for the region bounded by 25N–35N and 125E–135E, 32 percent of the 81 cyclone positions were of the 'small typhoon' classification. For the entire basin for the month of August, small typhoons comprise 15 percent of the total, and on a yearly basis they account for only 10 percent. Arakawa attributed their formation to the convergence zone which develops when the western end of

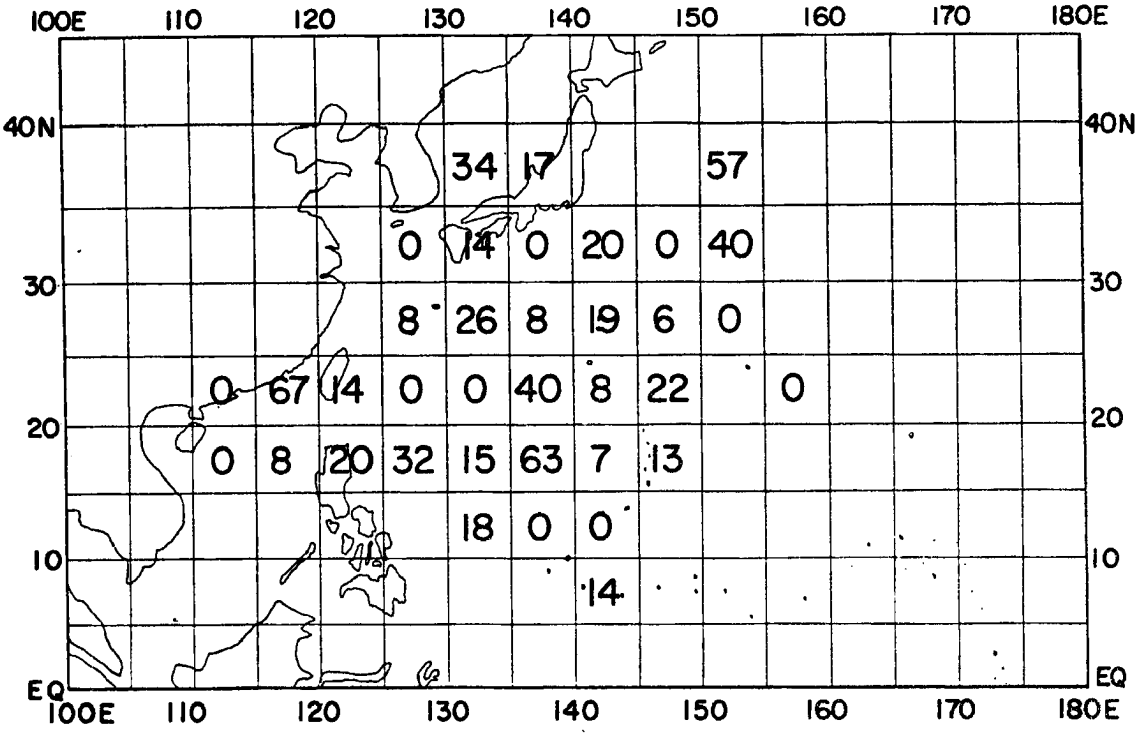

Fig. 14. Percent of cyclones per 5° latitude-longitude which fall into the 'large' category. Sample includes all August tropical cyclones, 1961-1969.

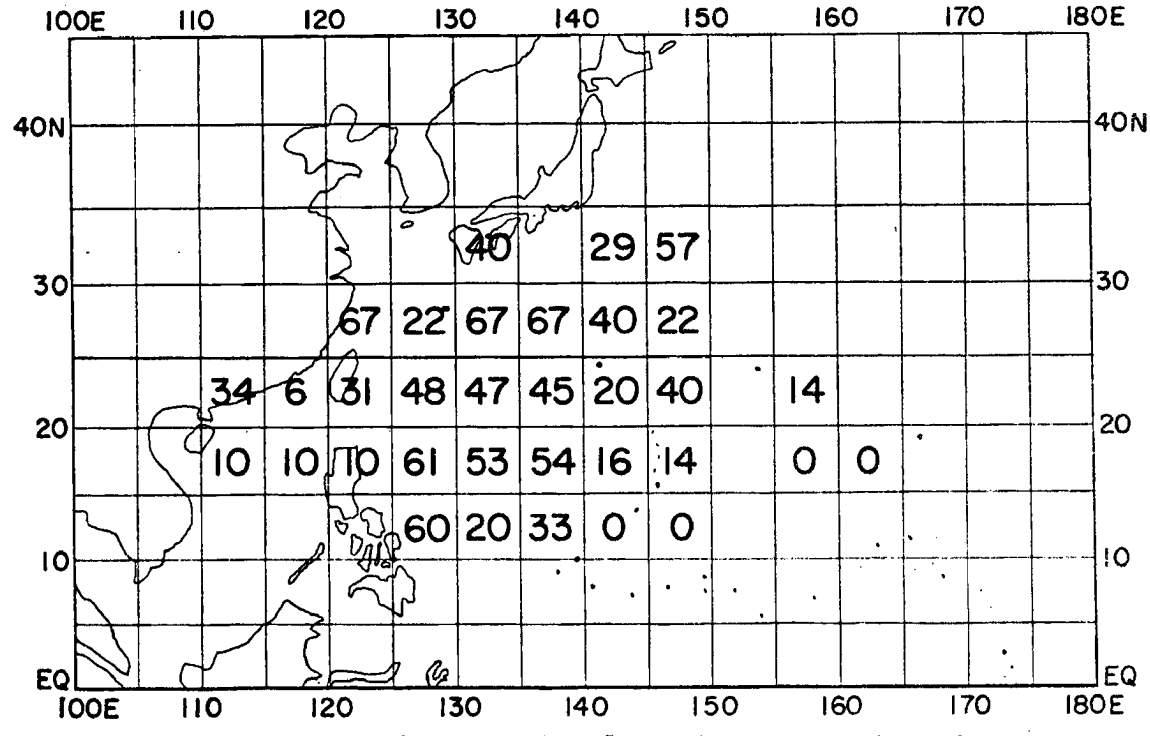

Fig. 15. Same as Fig. 14 except for September tropical cyclones.

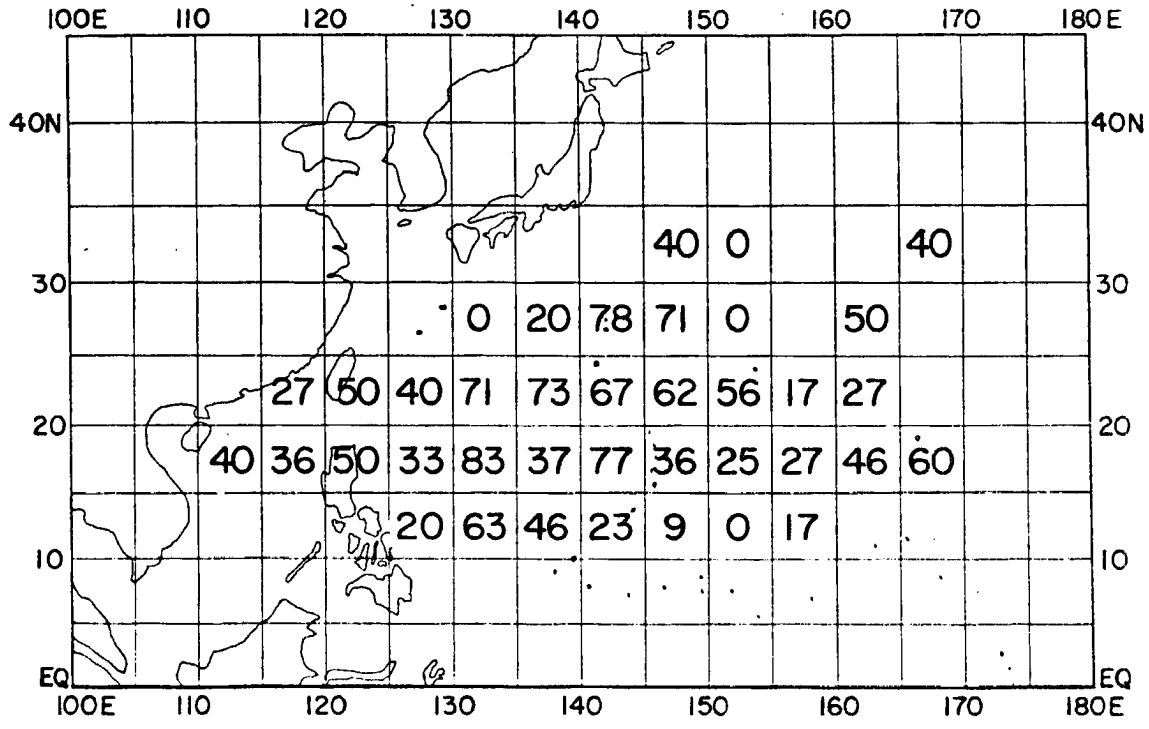

Fig. 16. Same as Fig. 14 except for October tropical cyclones.

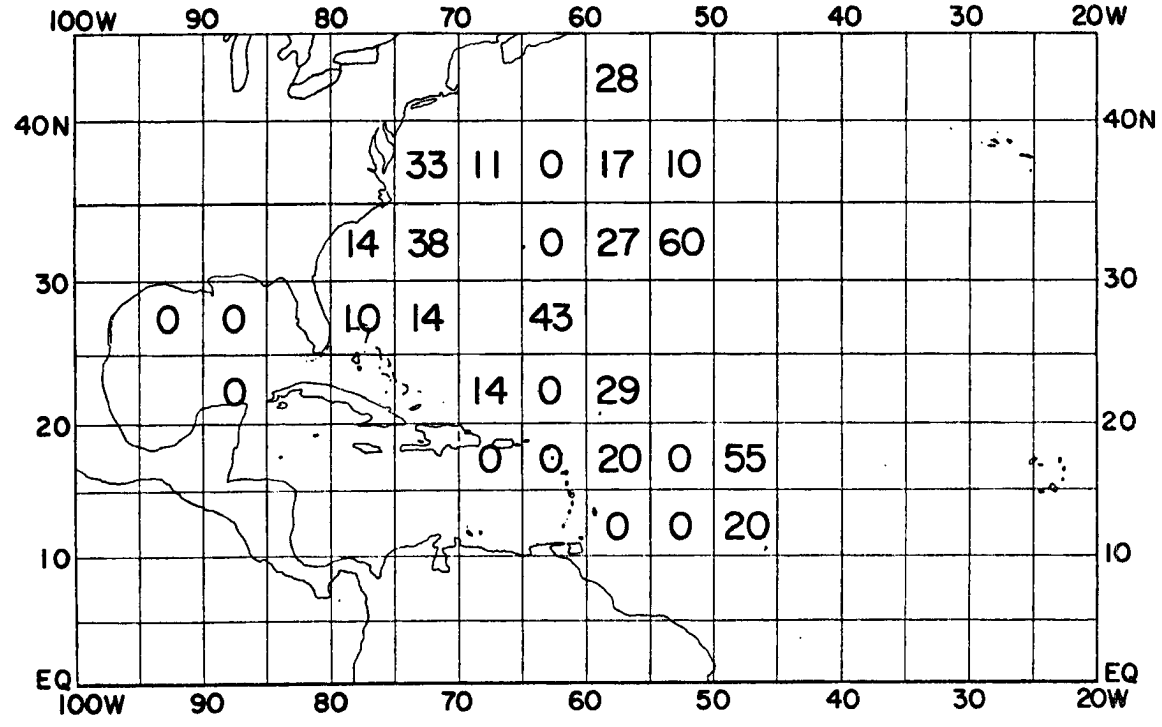

Fig. 17. Same as Fig. 14 except for large August cyclones in the Atlantic basin, 1957-1977.

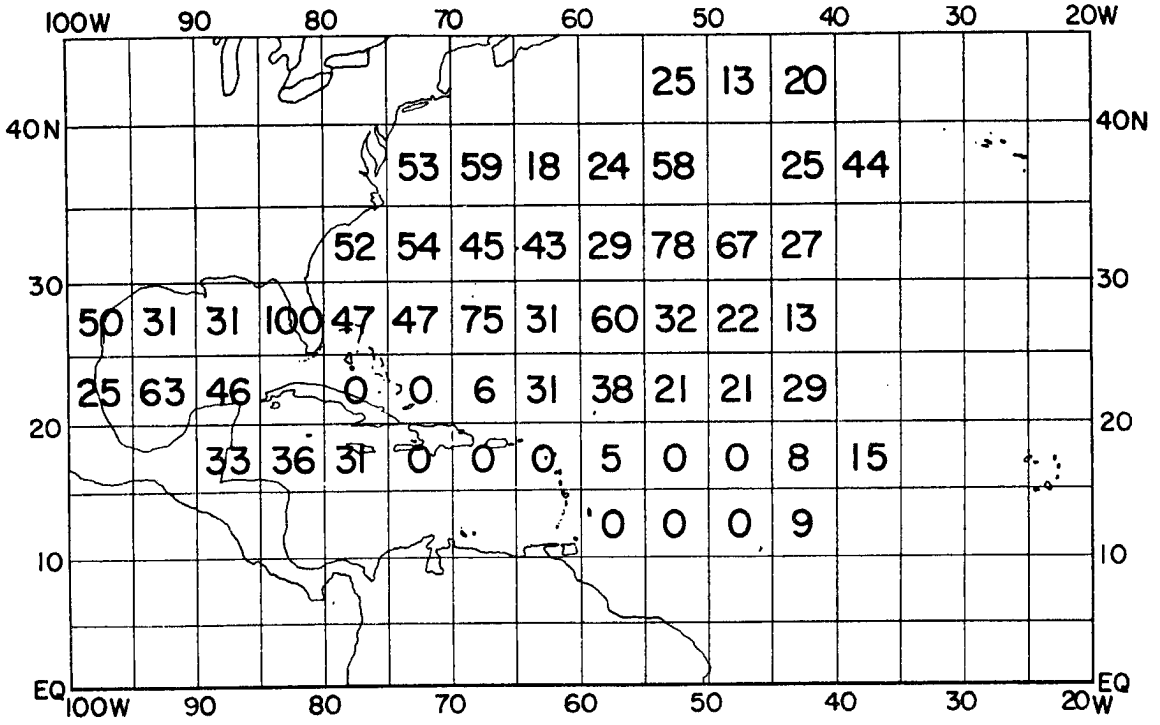

Fig. 18. Same as Fig. 17 except for September tropical cyclones.

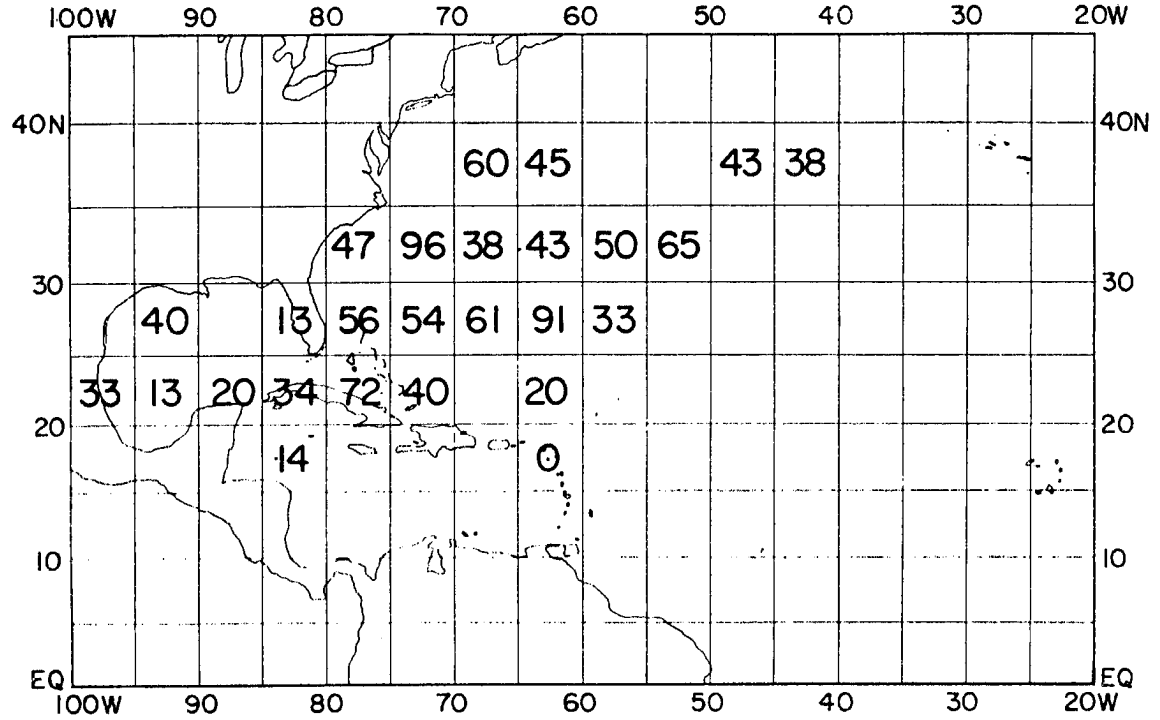

Fig. 19. Same as Fig. 17 except for October tropical cyclones.

the subtropical ridge fractures and drifts northwestward over the Sea of Japan. The result is a convergent but low-vorticity environment which spawns the small typhoons. The more frequent occurrence of large cyclones east of the Philippines corresponds with the typical location of the monsoon trough, which tends to develop cyclones of relatively large size.

Figure 15 shows frequencies of large cyclones for September. In contrast with August, the area south of Japan is dominated by large cyclones, and the high-frequency region associated with the monsoon trough has become more pronounced. The only areas where large cyclones are relatively rare are the South China Sea and the area south of 20N and east of 140E. The change in the frequency of large cyclones in the area south of Japan is thought to be associated with the reversal of the low-level flow which occurs over east Asia beginning in September; the area changes from a region of low vorticity on the margin of a subtropical high to a region of high vorticity between the subtropical ridge and a developing polar high over the continent. By October, 'the month of large cyclones', the region of maximum frequency has shifted southeastward, as the cold surges off of Asia become more frequent and powerful (Fig. 16). Brand (1972) describes an area bounded by 15N-25N and 140E-145E as a preferred area for very large typhoons having a ROCI of 10 degrees or more. The frequency of large typhoons (ROCI $\geq$ 6 degrees) in this area based on the 1961-1969 sample is 64 percent, as compared with a monthly percentage for the whole basin of 32 percent and a yearly average of 17 percent.

Atlantic. The frequency pattern of large cyclones for the Atlantic basin evolves in a similar fashion, but with one important difference:

the absence of a monsoon trough means that large cyclones are relatively rare south of 20N in all months. In August (Fig. 17), the pattern is somewhat erratic, but large cyclones are most frequent in the subtropical Atlantic from 30N to 35N. Of the 19 cyclone cases in the Gulf of Mexico during August, none were large. This area is similar to the small-typhoon region south of Japan, in that the environmental flow is anticyclonic, southerly and relatively weak. In September (Fig. 18) large cyclones become more frequent over the entire basin but particularly in the subtropical Atlantic from 25N-40N. As in the Pacific, this area begins to be affected by polar outbreaks during September, resulting in a high-vorticity environment. Unlike the Pacific, the Atlantic has no monsoon trough in September, and the tropics south of 20N rarely experience a large cyclone. Note the change of large cyclone frequency from south of 20N (rare) to north of 20N (frequent). In October (Fig. 19) the preferred genesis area shifts out of the central tropical Atlantic into the western Atlantic and northwest Caribbean where a monsoon trough is occasionally observed, and large cyclone activity reaches a maximum in an area somewhat to the south of the high frequency area of September.

Examination of the maps of frequency of large cyclones has yielded evidence that large and small cyclones are clustered in space as well as time, and that the clustering is consistent in both the Atlantic and Pacific basins. An increase in the frequency of large cyclones is observed in early autumn as the environment over the western oceans changes from anticyclonic to cyclonic with the beginning of cold outbreaks from the continents of Asia and North America. Section 3.5

will present some typical cyclone life histories and summarize the climatology of large and small tropical cyclones.

3.4 The Relationship Between Size and Intensity

It was mentioned in the introduction and again earlier in this chapter that cyclone size cannot be explained totally in terms of cyclone intensity, although the two are related. This is illustrated in Figs. 20 and 21, which show size as a function of maximum wind for the 21 year Atlantic and 9 year Pacific cyclone samples respectively. Also plotted is the least-squares regression line computed from the size and maximum wind. A linear relationship does exist, but the percentage of variance explained by it (around 10% in both cases) is small.

In the short term, particularly in the early stages of vortex development, Zipser (1964) noted that small cyclones tended to intensify more rapidly than weaker ones, at least for the 13 cases he examined. The climatological data studied here did not reveal a general difference of intensity change between large and small cyclones.

3.5 Characteristic Changes in Tropical Cyclone Size and Intensity

Thus far we have viewed tropical cyclone size as static - in terms of occurrence in given locations and at given times. However, as with all cyclone parameters, it changes as the cyclone moves through different environments. Three collections of time series of cyclone size are shown in Figs. 22-24. Figure 22 shows the evolution of size of relatively large Atlantic cyclones with a ROCI of 4^{o} or more when they first reach hurricane intensity. During the first several days, most of them contract toward the basin mean value of 3^{o}. Figures 23 and 24 both show the changes of size of small hurricanes which start with a ROCI of 2^{o} or less, with one difference - Fig. 23 is composed only of hurricanes

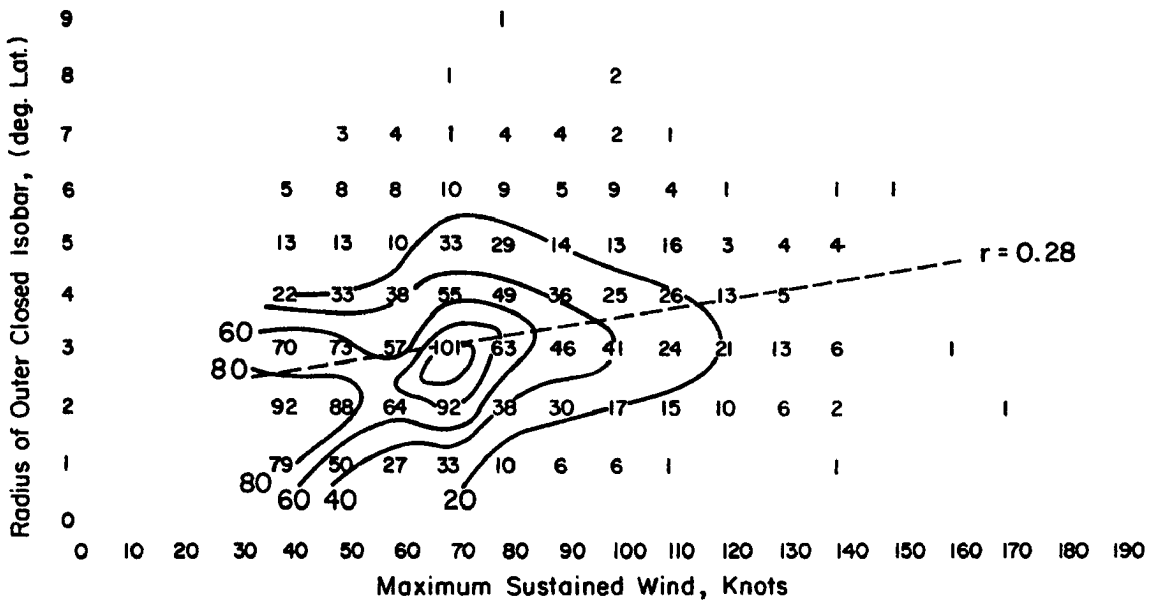

Fig. 20. Tropical cyclone size as a function of maximum sustained wind for Atlantic tropical cyclones, 1957-1977. Observations are tabulated in classes of 1° latitude and 10 kts. The least square line is fitted to the raw data.

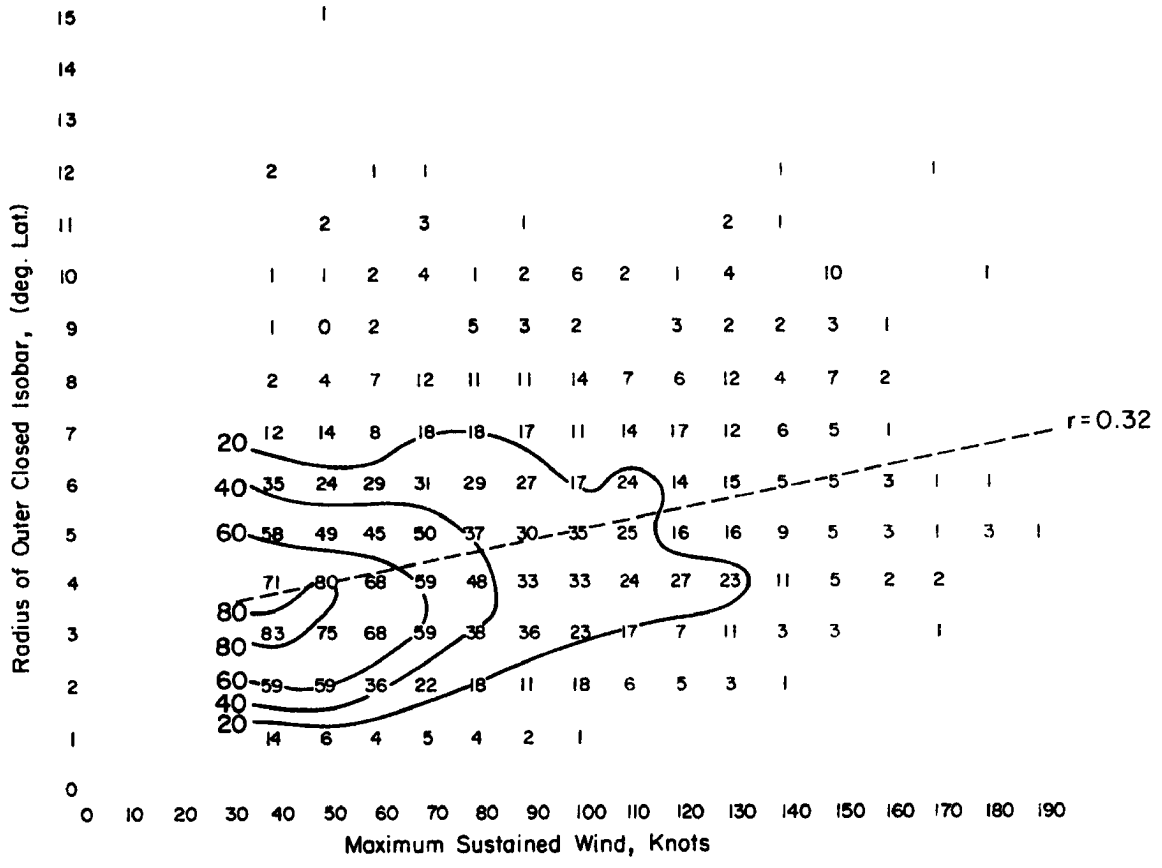

Fig. 21. Same as Fig. 20 except for Pacific tropical cyclones.

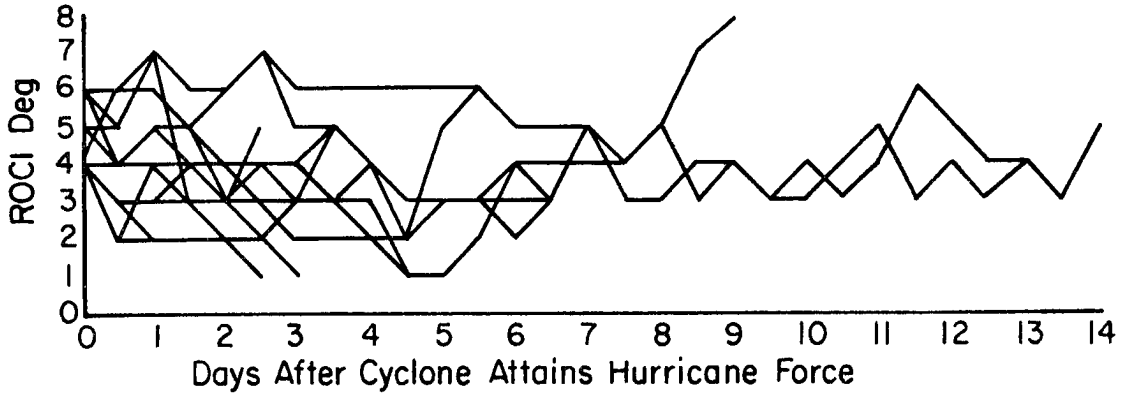

Fig. 22. Changes in size of large hurricanes with an initial ROCI of 4° latitude or more.

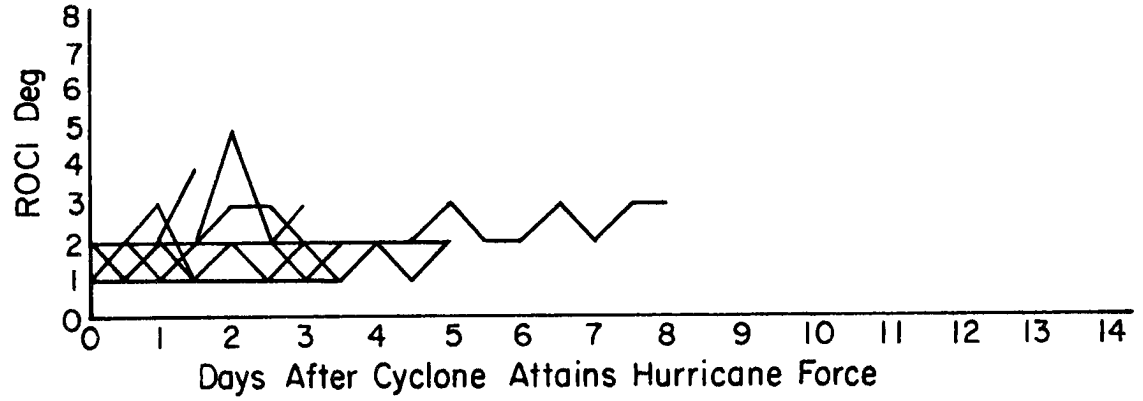

Fig. 23. Changes in size of small westward-moving hurricanes with an initial ROCI of 2° latitude or less.

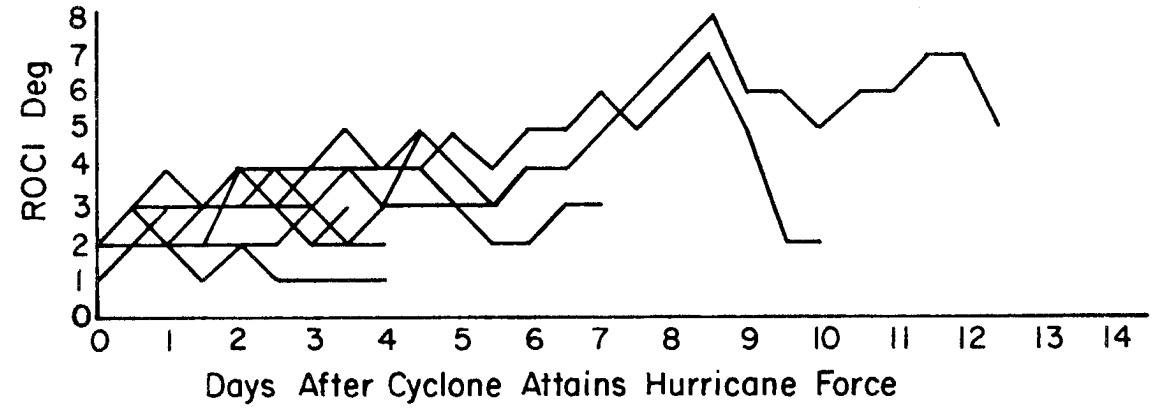

Fig. 24. Changes in size of small, recurving or eastward moving hurricanes with an initial ROCI of 2° latitude or less.

which moved predominantly westward, while Fig. 24 is of recurving and eastward-moving hurricanes. Westward-moving Atlantic hurricanes (Fig. 23) which begin small tend to remain that way - they never leave the type of environment that spawned them. Recurving systems (Fig. 24) usually grow as they reach the subtropics.

The above implies a characteristic life cycle of hurricanes involving changes in size as well as intensity. Dunn and Miller (1960) and Riehl (1979) divided the life of the Atlantic hurricane into four idealized stages:

1) The formative stage -- a period from the development of the initial vortex to the first occurrence of hurricane force winds. The cyclone typically contracts slightly and develops the characteristic high-energy core during this stage.
2) The immature stage -- a time of rapid intensification with only a very slight change in size. The maximum wind of the cyclone's life is attained at the end of this stage.
3) The mature stage -- the cyclone begins to grow during this stage, but is no longer increasing in intensity. Most of the severe hurricanes affecting the United States are in this stage.
4) The decaying stage -- a period when the cyclone reaches its greatest size and begins to collapse, while the maximum winds diminish.

Such a model of hurricane evolution is useful even though there are many exceptions to it during an actual cyclone season. Using the cyclone size and position data, more quantitative versions of this and

other cyclone life cycles can be prepared by averaging cyclones of a characteristic type. Three are presented here: 1) recurving Atlantic hurricane, 2) October hurricane and 3) October supertyphoon.

The recurving Atlantic hurricane (Fig. 25) follows the life cycle as described by Riehl. Twelve hurricanes which formed in the central Atlantic and attained maximum winds of at least 45 m s^{-1} were averaged together to determine wind and size on successive days after formation. The cyclone forms with a ROCI of 2.5 degrees and remains at about the same size for 3.5 days, and then grows slightly to 4 degrees as it reaches its maximum winds of 60 m s^{-1}. It attains a maximum size of 5 degrees one half day after recurvature and 7.5 days after genesis as its winds drop to around 35 m s^{-1}. Note that the increase in size commences as the cyclone turns northward, typically into a slowly-moving trough in the westerlies associated with a polar high over the eastern United States.

Figure 26 is a composite of six October hurricanes. Occasionally in June or October the intertropical convergence zone shifts far enough to the north in the western Caribbean Sea to acquire the cyclonic lower tropospheric flow characteristic of a monsoon trough, and a cyclone of this type may develop. They may on occasion become quite severe, but most typically reach maximum winds of 45 m/s or less, and remain at nearly the same size or even contract slightly as they move into the Atlantic. Their usual genesis size of 4 degrees is large for the Atlantic.

Figure 27 shows the October supertyphoon, characteristically the largest and most powerful tropical cyclone on earth. This cyclone is based on an average of 6 typhoons with central pressures below 930 mb.

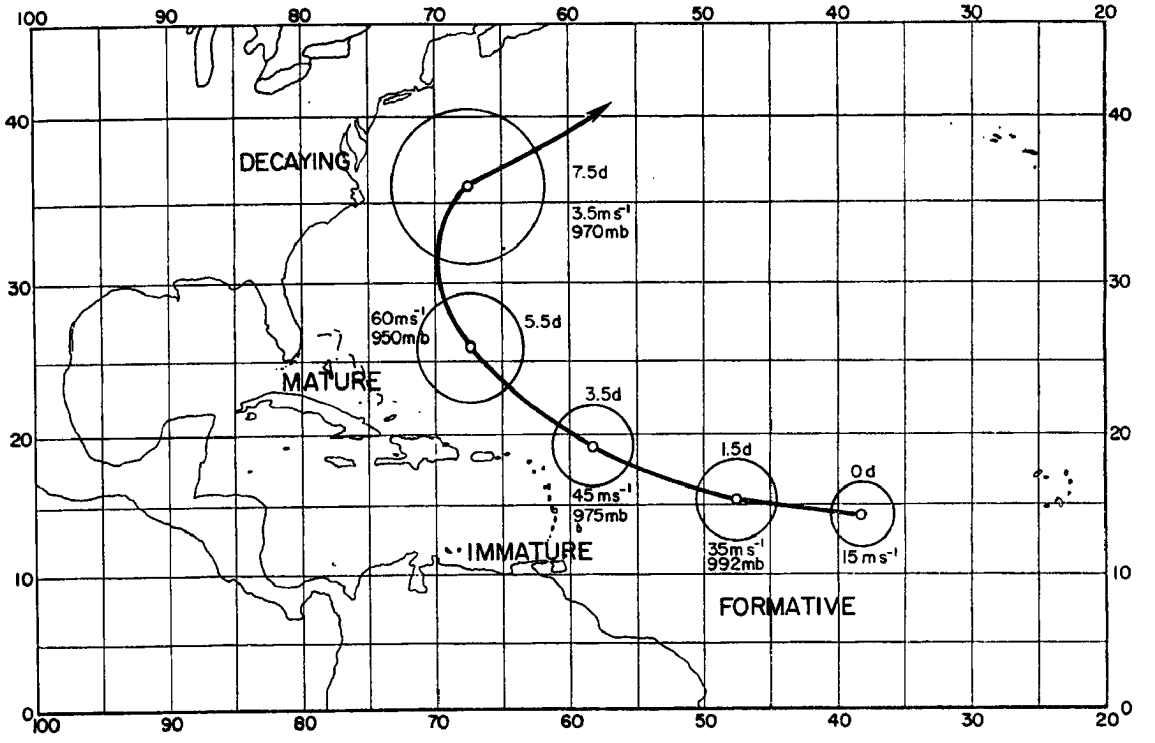

Fig. 25. Average changes of size and intensity of 12 recurving Atlantic hurricanes. The circle has the same radius as the average outer closed isobar.

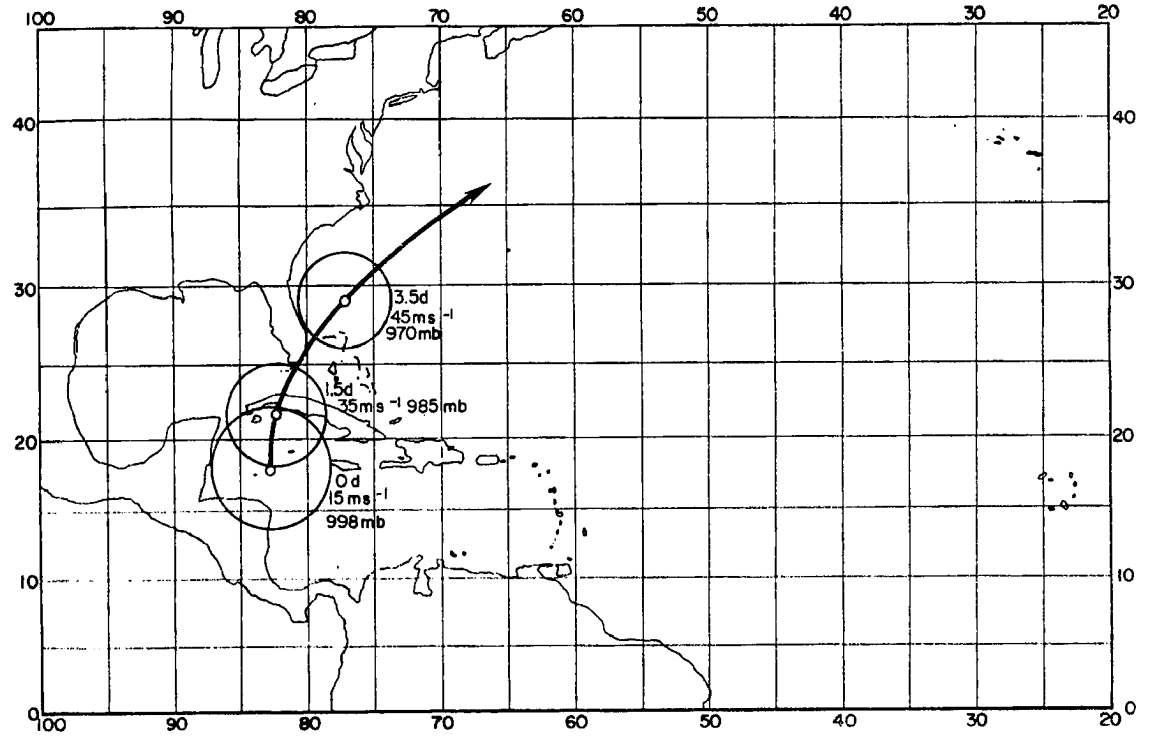

Fig. 26. Same as Fig. 25 except for the six October hurricanes.

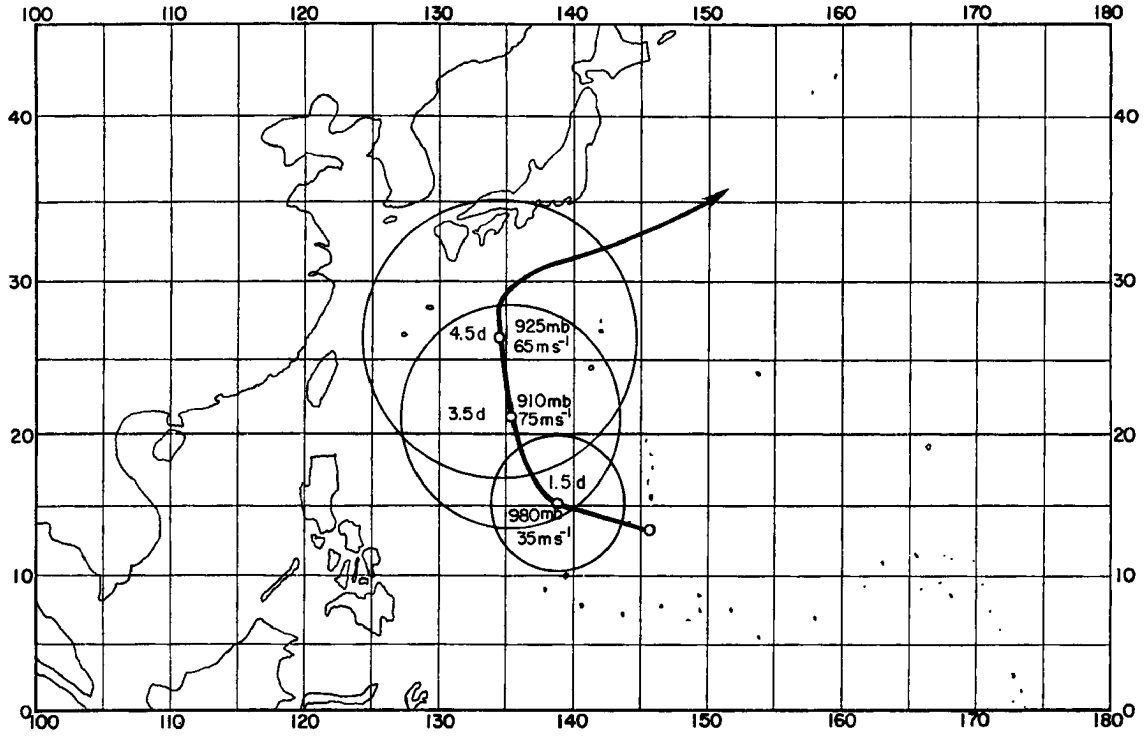

Fig. 27. Same as Fig. 25 except for six October supertyphoons.

It forms at a size of 5 degrees in the monsoon trough, and simultaneously deepens rapidly to 910 mb and grows to 8 degrees. Peak winds reach about 75 m s^{-1}. At recurvature it has a ROCI of 10 degrees and winds of about 65 m s^{-1}.

These three life cycles are a very limited representation of the patterns that can evolve. Some of the general conclusions resulting from the climatology of large and small tropical cyclones are listed below.

1) Typhoons and Pacific tropical storms are over twice as large as their Atlantic counterparts when the area enclosed by the outer closed isobar is considered.

2) A consistent, seasonal progression in tropical cyclone size, with a midsummer minimum and fall maximum, is present in both ocean basins.

3) Large cyclones are more frequent in particular regions within the basin where the lower-tropospheric vorticity of the environment is relatively large -- in the vicinity of the monsoon trough or between the subtropical ridge and the polar anticyclones which begin to develop over the eastern United States and China during early autumn.

4) Conversely, small cyclones are more frequent in areas of minimum environmental vorticity — the trade easterlies of the tropical Atlantic and Pacific, and the subtropical ridge margins of the midsummer Gulf of Mexico and extreme western Pacific Ocean.

4. STRUCTURE OF LARGE AND SMALL TROPICAL CYCLONES

4.1 Introduction

The previous chapter addressed the first task of this paper by presenting a climatology describing the variability of tropical cyclone size both temporally and spatially. This chapter discusses the structural aspects of cyclone size, including mean wind fields based on rawinsonde compositing methods, differences between mean cyclones of different sizes, basins, and intensities, statistical support for these differences and some approximate spatial distributions of 15 m s^{-1} surface winds.

The rawinsonde compositing method used in this work has been in use on Professor Gray's tropical cyclone research project for several years. For each cyclone position, all available rawinsonde soundings within 15^{o} latitude are navigated onto a polar-coordinate grid centered on the cyclone. The basic grid (Fig. 28) consists of 8 octants subdivided into 8 belts. For wind compositing, the grid may be positioned in two ways - geographically, with octant 1 always to the north, or relative to the cyclone, with octant 1 centered on the cyclone motion vector. The winds themselves can also be modified by subtracting out the cyclone motion vector. Four wind composites result: 1) Natural, or NAT - geographic grid and total winds, 2) Motion, or MOT - geographic grid and relative winds (cyclone motion removed), 3) Rotated or ROT - rotated grid and natural winds, and 4) MOTROT - rotated grid and relative winds. This

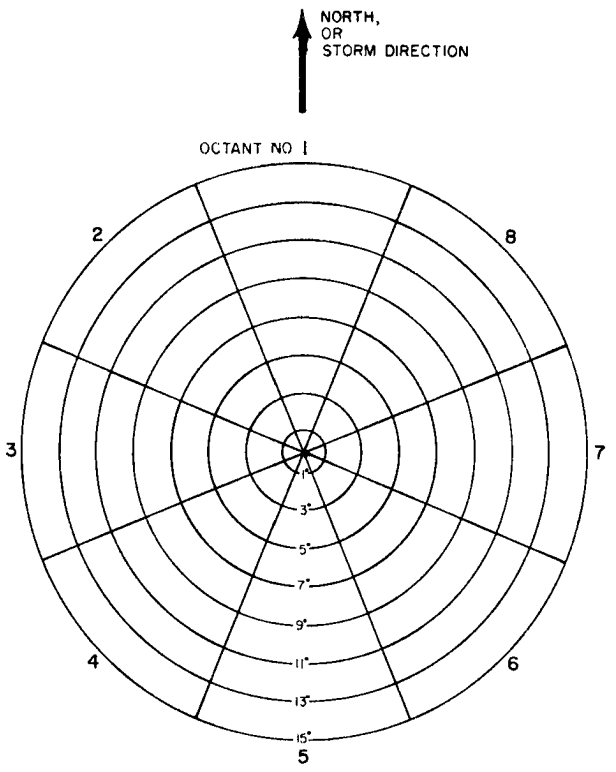

Fig. 28. Grid used in compositing rawinsonde observations around tropical cyclones.

rawinsonde compositing method has been extensively documented by Gray et al. (1982). The grid is repositioned for each cyclone central position, and an average is computed for each sounding parameter at each of 21 pressure levels from the surface to 50 mb using all soundings in each grid region.

Rawinsonde composites were made for 11 mutually exclusive cyclone position sets from Atlantic and Pacific in order to detect systematic differences between large and small tropical cyclones. The six stratifications for the Pacific are identical to those used to study the climatology. The Atlantic composite stratifications have been modified somewhat. Stratifications for both basins are listed in Table 5. The changes in the Atlantic stratifications from those used in the

TABLE 5

Stratification criteria for large and small tropical cyclones.

ATLANTIC		
Small/Medium Tropical Storm	$R \leq 3^{o}$	$17 \text{ m s}^{-1} \leq V_{max} < 33 \text{ m s}^{-1}$
Large Tropical Storm	$R \geq 4^{o}$	$17 \text{ m s}^{-1} \leq V_{max} < 33 \text{ m s}^{-1}$
Small/Medium Hurricane	$R \leq 3^{o}$	$V_{max} \geq 33 \text{ m s}^{-1}$
Large Hurricane North	$R \geq 4^{o}$	$V_{max} \geq 33 \text{ m s}^{-1}$ LAT > 25N
Large Hurricane South	$R \geq 4^{o}$	$V_{max} \geq 33 \text{ m s}^{-1}$ LAT $\leq$ 25N
PACIFIC		
Small Tropical Storm	$R < 3^{o}$	MSLP > 980 mb
Medium Tropical Storm	$4^{o} \leq R \leq 5^{o}$	MSLP > 980 mb
Large Tropical Storm	$R \geq 6^{o}$	MSLP > 980 mb
Small Typhoon	$R \leq 3^{o}$	MSLP $\leq$ 980 mb
Medium Typhoon	$4^{o} \leq R \leq 5^{o}$	MSLP $\leq$ 980 mb
Large Typhoon	$R \leq 6^{o}$	MSLP $\leq$ 980 mb

climatological study were to allow comparisons between Atlantic and Pacific cyclones after the influence of size differences have been removed.

4.2 Mean Structural Differences Between Large and Small Tropical Cyclones

The azimuthally averaged tangential winds in NAT coordinates for four Atlantic and four Pacific composites are shown in the Appendix. All are qualitatively similar - a maximum in tangential winds at small radii and in the low to middle troposphere, decreasing upward and becoming negative in the upper troposphere. The intercomparisons which can be made are quite numerous, but will here be limited to three types: 1) comparisons of cyclones of equivalent intensity and differing size, 2) comparisons of cyclones of equivalent size and differing intensity, and 3) comparisons of cyclones of equivalent size and intensity from

different basins. Differences in strength are not treated explicitly but are apparent in many of the comparisons.

Figures 29-32 show difference fields between cyclones of different size but equivalent intensity. With the exception of the Atlantic large hurricane minus the small/medium hurricane, the maximum tangential wind differences lie in the low and middle troposphere at radii of 4^{o} to 6^{o} latitude. In all cases the wind differences in this region exceed 5 m s^{-1} - roughly equivalent to a doubling of wind speeds in this area.

Tangential wind difference fields for cyclones of different intensities (Figs. 33-36) reveal the structural implications of size differences and intensity differences. Differences in tangential wind in excess of 5 m s^{-1} are here confined to the region inside 3^{o} (4^{o} for large typhoon minus small typhoon), and changes from $4-6^{o}$ are on the order of only 2.5 m s^{-1}. Even at 2^{o} radius, where the typical difference is about 7.5 m s^{-1} a change of only 20%-40% is observed. When it is then considered that the area from $4-6^{o}$ radius is over twice as large as the area from $0-3^{o}$ radius, the importance of the wind differences for cyclones of different sizes becomes apparent. Some of the implications of cyclone size on cyclone dynamics will be addressed in Chapter 5.

A by-product of these size-based composites is the first opportunity to compare hurricanes and typhoons after the size difference has been eliminated. Figure 37 shows the difference between the small/medium hurricane and small typhoon - both have a ROCI of $1-3^{o}$. Most of the difference indicates that the small/medium hurricane is of

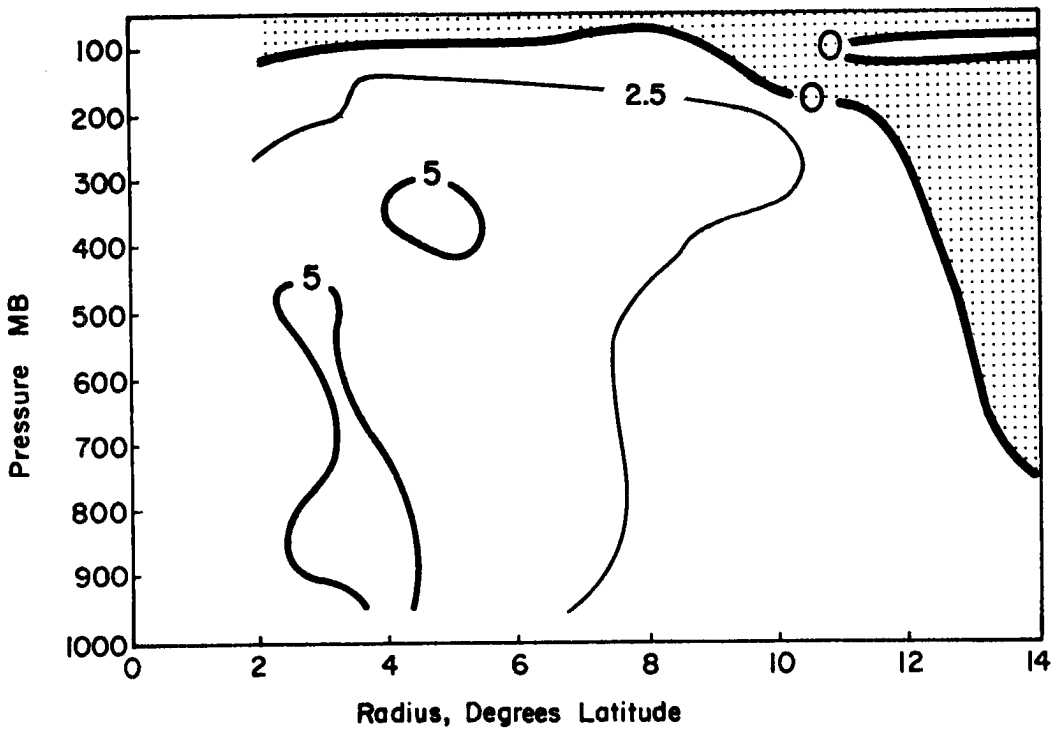

Fig. 29. Difference of azimuthal mean tangential wind, Atlantic large tropical storm minus Atlantic small tropical storm.

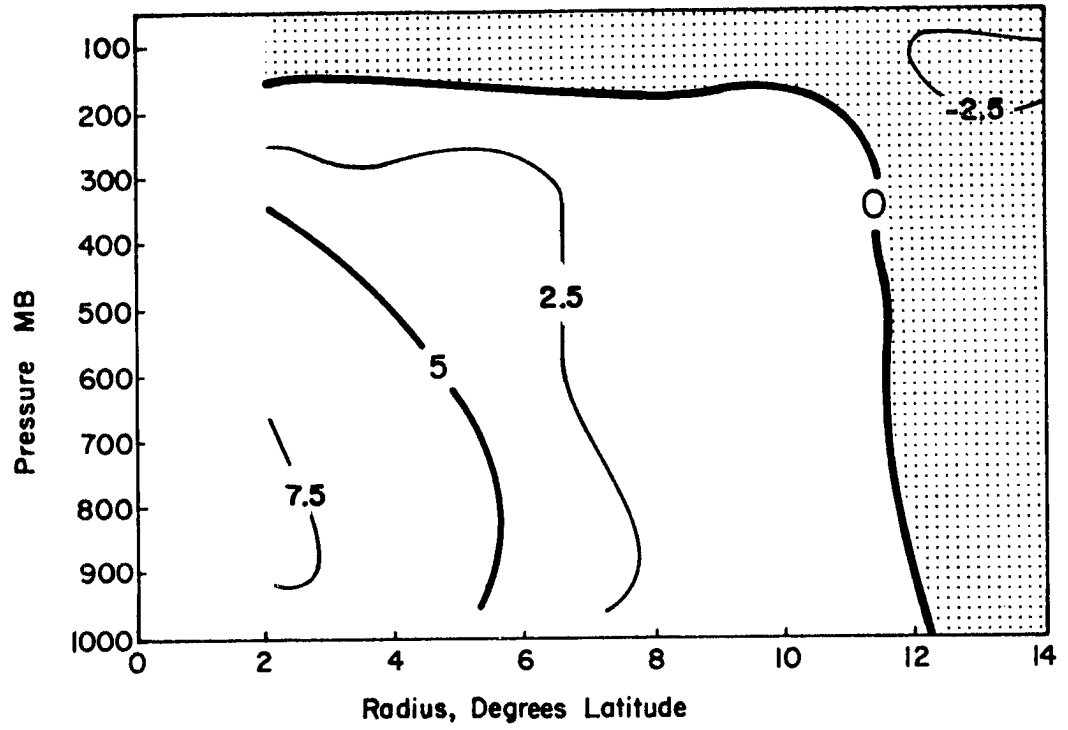

Fig. 30. Same as Fig. 29 except for Atlantic large hurricane north minus small/medium hurricane.

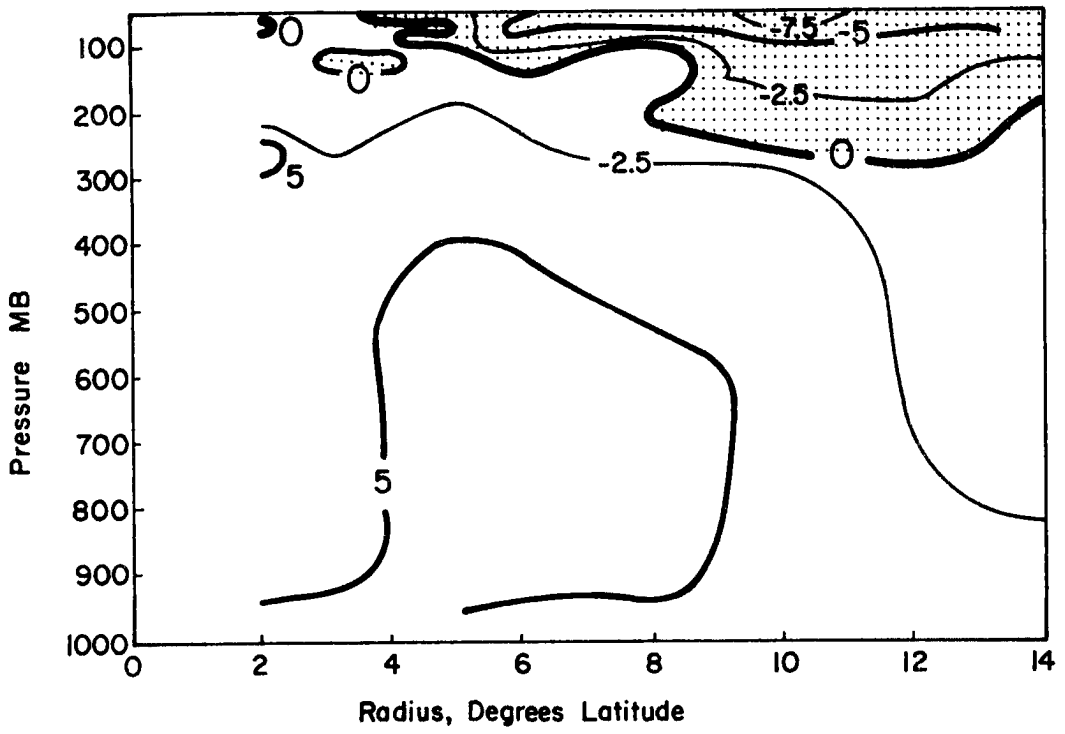

Fig. 31. Same as Fig. 29 except for Pacific large tropical storm minus small tropical storm.

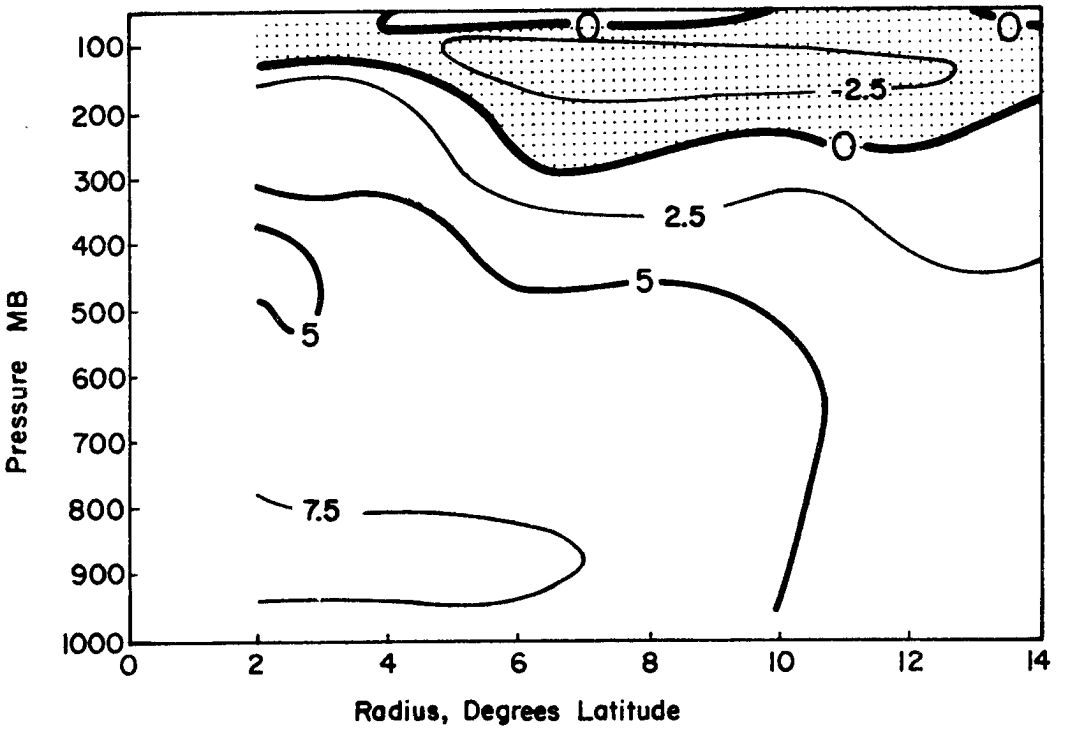

Fig. 32. Same as Fig. 29 except for Pacific large typhoon minus small typhoon.

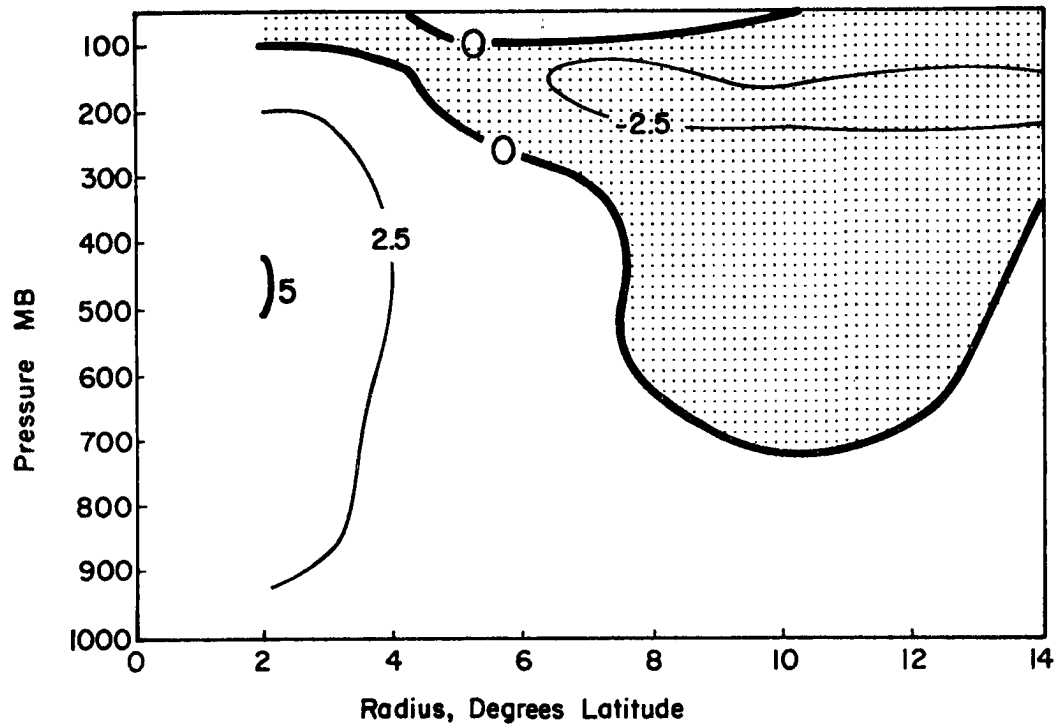

Fig. 33. Same as Fig. 29 except for Atlantic small/medium hurricane minus small tropical storm.

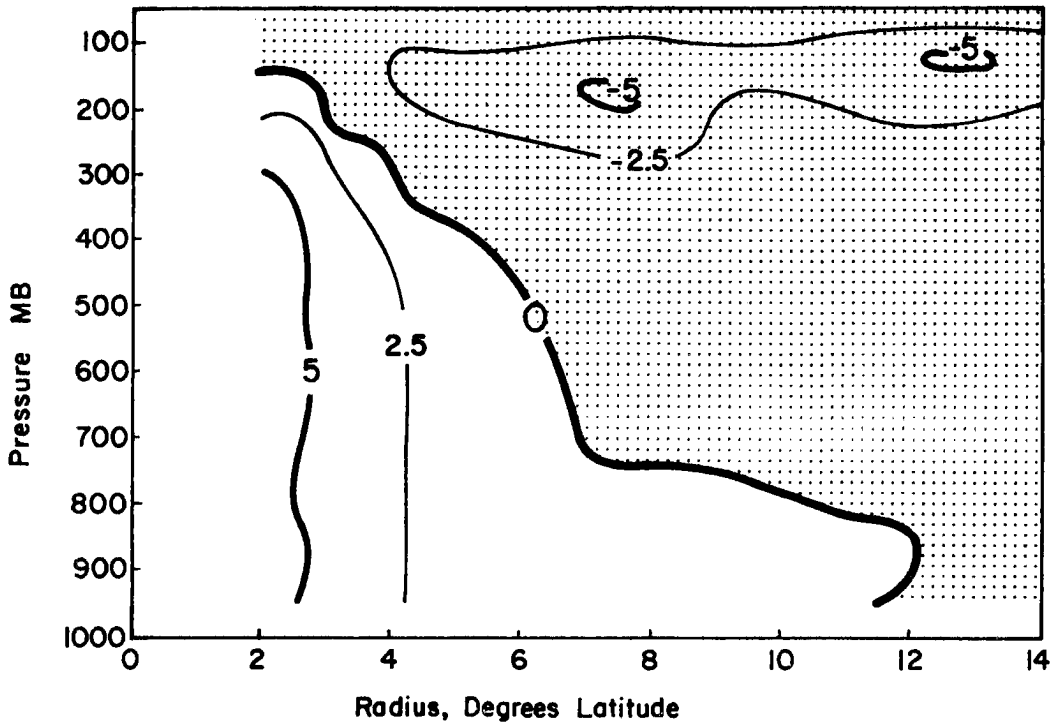

Fig. 34. Same as Fig. 29 except for Atlantic large hurricane north minus large tropical storm.

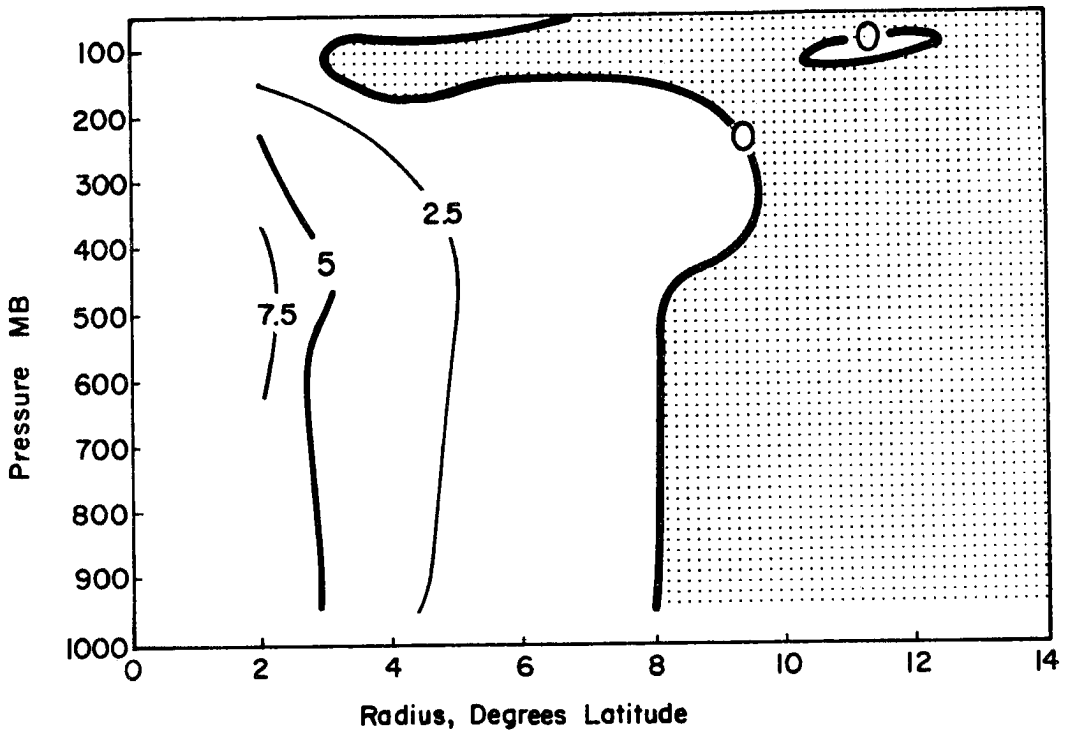

Fig. 35. Same as Fig. 29 except for Pacific small typhoon minus small tropical storm.

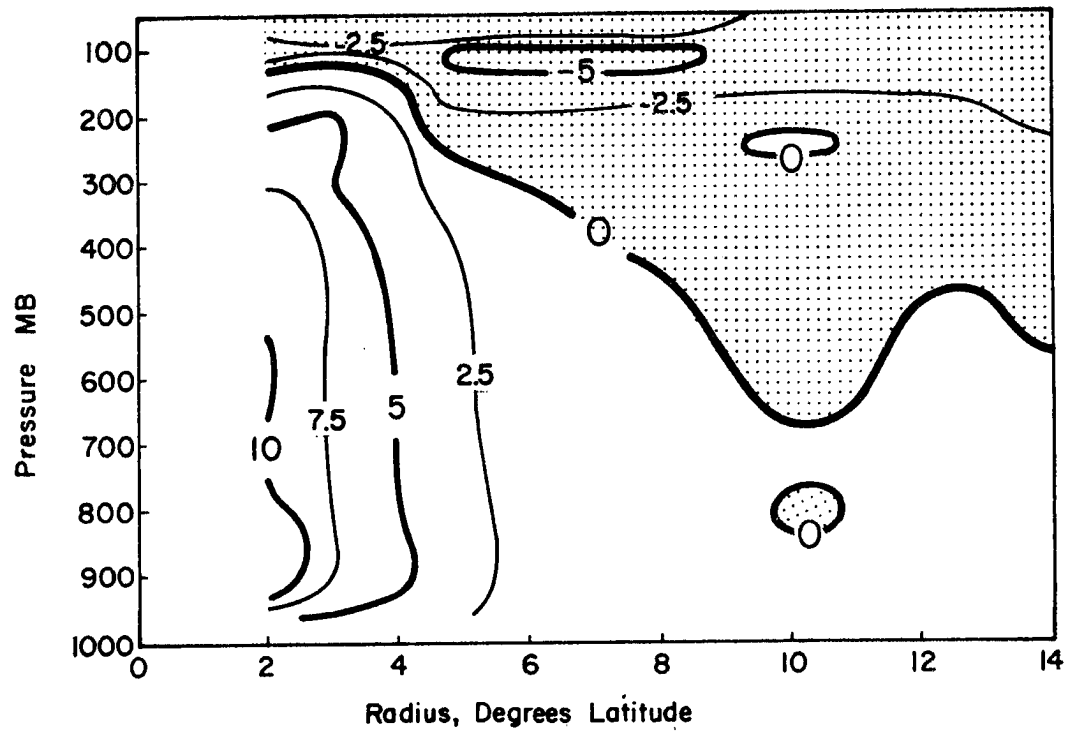

Fig. 36. Same as Fig. 29 except for Pacific large typhoon minus large tropical storm.

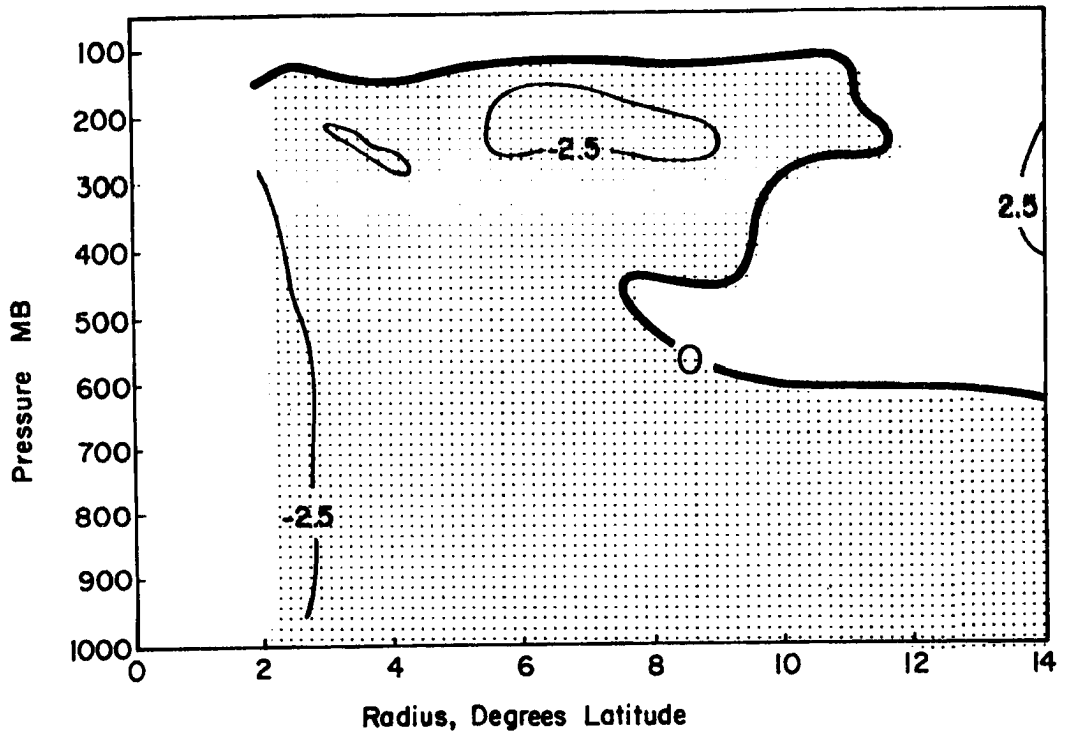

Fig. 37. Same as Fig. 29 except for Atlantic small/medium hurricane minus Pacific small typhoon.

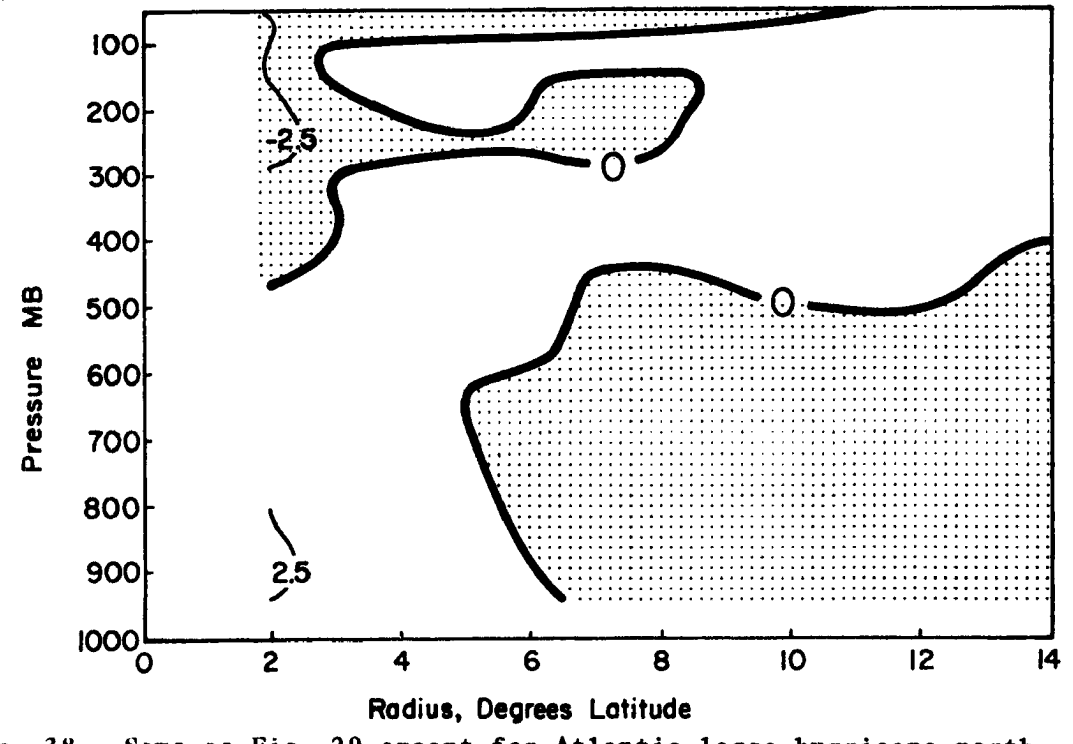

Fig. 38. Same as Fig. 29 except for Atlantic large hurricane north minus Pacific medium typhoon.

lesser intensity. Figure 38 compares the large hurricane north with a medium typhoon - again both systems are of equivalent size and the differences are mainly apparent inside 2^{o} radius.

4.3 Statistical Significance of Tangential Wind Differences

One criticism leveled at the rawinsonde compositing method in the past is that formal assessment of the statistical significance of the differences of means was seldom made. Because this paper uses an indirect definition (the outer closed isobar measurement) to estimate the size of the wind field, statistical support of the wind differences is even more important.

The 850 mb winds are examined because they can be related to surface winds (Frank and Gray, 1980). From the 850 mb wind distributions it is possible to make not only statistical calculations but also frequency-of-occurrence tables for surface wind speeds above a threshold value.

The tangential winds at 850 mb are tabulated for all 8 octants and 8 belts in the ROT coordinate system for each Atlantic composite. Because the rawinsonde stations are not evenly distributed, some of the octants in the rawinsonde composites have more observations than others. This complicates the statistical analysis. Adding all of the tangential wind observations together and dividing by the total to get a mean will give a biased result; the type of bias depends on where most of the observations were. If most of the observations were to the right of the cyclone (where the tangential wind is usually stronger) this mean would be larger than the mean obtained if the belt were sampled perfectly and the observations were thus evenly distributed over all octants. It is

important that each octant, rather than each observation, is weighted equally. A method for combining, or 'pooling', the observations in this manner is described below.

The approach used is to weight individual observations more heavily in octants where they are less numerous. Wind data are tabulated into classes of 1 m s^{-1} width (say, 6 m $s^{-1} \leq v < 7$ m s^{-1}) for each octant and belt in the composite grid (Fig. 28). The result is an array of frequencies $n_{i,j,k}$; each frequency is the number of observations in octant i (1 through 8) and belt j (1 through 8) which fell into speed class k. For a particular belt and octant, adding all of the $n_{i,j,k}$ together gives the total number of observations in octant i and belt j, designated by $M_{i,j}$. What is desired is a combination of all octant values of $n_{i,j,k}$ for a particular belt; the result $F_{j,k}$ is the pooled frequency of observations of wind class k in belt j, and is given by Eq. 1,

$$F_{j,k} = \sum_{i=1}^{Oct} n_{i,j,k} W_{i,j} \tag{1}$$

where the weighting factor $W_{i,j}$ is given by

$$W_{i,j} = \begin{cases} \dfrac{\sum_{i=1}^{8} M_{i,j}}{(M_{i,j})(Oct)} & M_{i,j} \neq 0 \\ 0 & M_{i,j} = 0 \end{cases} \tag{2}$$

where

$F_{j,k}$ = pooled frequency of kth wind class in jth belt

Oct = number of octants with at least 1 wind measurement (equal to 8 except at inner radii where some octants have no data)

$n_{i,j,k}$ = number of winds of class k in ith octant and jth belt

$W_{i,j}$ = weighting factor for ith octant observations used to compute jth belt pooled distribution

$M_{i,j}$ = number of observations in ith octant and jth belt,

$$= \sum_{\text{all } k} n_{i,j,k}$$

computed from the distribution of observations $M_{i,j}$ using Eq. 2. Application of Eq. 1 to all wind classses (the weighting factors for a given octant and belt need be computed only once at each level) gives a frequency distribution of tangential wind for belt j. The mean and standard deviation of this distribution can then be calculated in the usual way. Equation 3 gives an expression for the mean of the pooled distribution. This mean is the same as that obtained by averaging all of the octant means together,

$$\bar{X}_{j \text{ pooled}} = \frac{\sum_{\text{all } k} F_{j,k} X_k}{\sum_{\text{all } k} F_{j,k}} = \frac{1}{\text{oct}} \bar{X}_{i,j} \qquad (3)$$

where

$\bar{X}_{j \text{ pooled}}$ = mean of variable x for belt j, based on the pooled distribution

$F_{j,k}$ = pooled frequency of wind class k in belt j

X_k = midpoint of class k (i.e. the wind class $6 \leq v < 7$ would have midpoint 6.5).

Figures 39 and 40 are prepared using the pooled frequency distributions of 850 mb tangential wind for 7 belts (the $0-1^{o}$ latitude belt is omitted because it contains so few observations). The means are computed using Eq. 3, and the 95% confidence limits for the means estimated by using the t-distribution and the standard deviations of the pooled distributions (Walpole and Myers, 1978). This test assumes that: 1) the observations making up the sample are independent and 2) the underlying population is normally distributed. Inspection of the distributions shows the second assumption to be quite good. The first is less accurate because some of the observations come from the same tropical cyclones. However, the differences between the means in Figs. 39 and 40 are so great that even using expanded confidence intervals to compensate for the dependence in the data would not affect the significance of the results.

4.4 Extent of 15 m s^{-1} (30 kt) Surface Winds

Cyclone size becomes an important practical consideration because of the extent of the surface wind field. Frank and Gray (1980) prepared a study of the frequency of occurrence of 15 m s^{-1} (30 kt) surface winds around tropical cyclones using rawinsonde compositing methods. They assumed the surface winds to be 75% of the 850 mb winds, and tabulated the frequency of occurrence of 20 m s^{-1} 850 mb winds around Atlantic cyclones of different intensities and Pacific cyclones of different intensities and sizes. They found that high winds at a given radius are more frequent for larger and more intense cyclones, and relatively more frequent on the right side of the vortex than on the left.

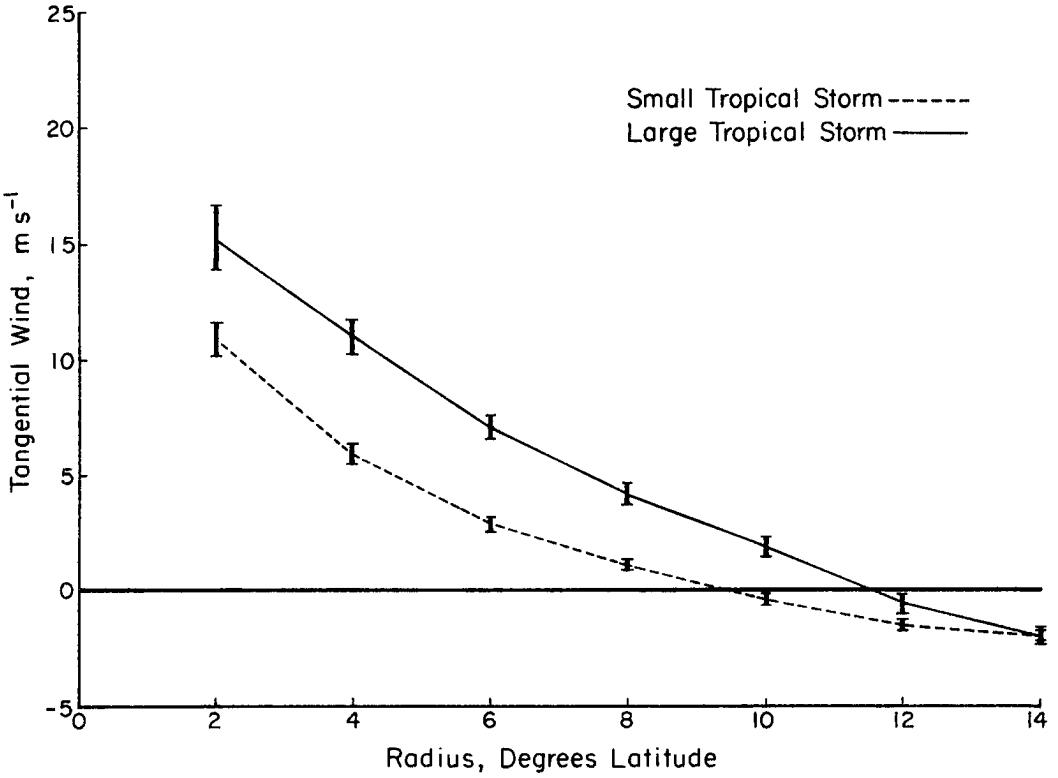

Fig. 39. Radial profile of azimuthal mean tangential wind for Atlantic tropical storms. Vertical bars denote the 95% confidence limits on the mean at each radius.

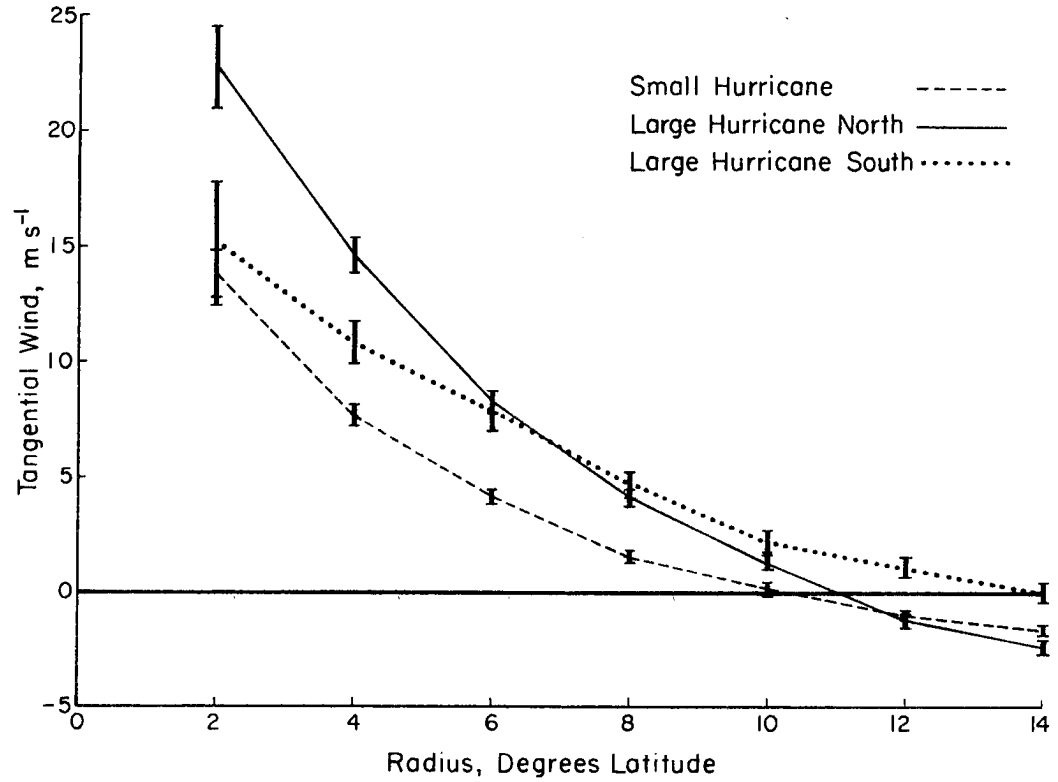

Fig. 40. Same as Fig. 39 except for Atlantic hurricanes.

Using the wind speed frequency distributions from the Atlantic rawinsonde composites described earlier in this chapter, the frequencies of 20 m s^{-1} 850 mb winds were computed for 1-3°, 3-5°, and 5-7° latitude radius for each octant. The results are plotted in Figs. 41-44. No values are shown inside 1° latitude where the number of observations is insufficient to obtain stable frequencies. The pattern which emerges is similar to that observed in the mean winds - high winds at a given radius are more frequent in large cyclones than small ones.

These wind fields were obtained from composites, but show the probability of encountering 15 m s^{-1} surface winds at various locations around individual cyclones of different sizes and strengths. With refinements such frequencies could aid forecasters in estimating the extent of gale force winds when central pressure and radius of outer-closed-isobar estimates are available. By compositing satellite winds and surface reports from ships, it might be possible to obtain a more detailed and finely stratified set of figures like these which would be of real value in forecasting and ship routing.

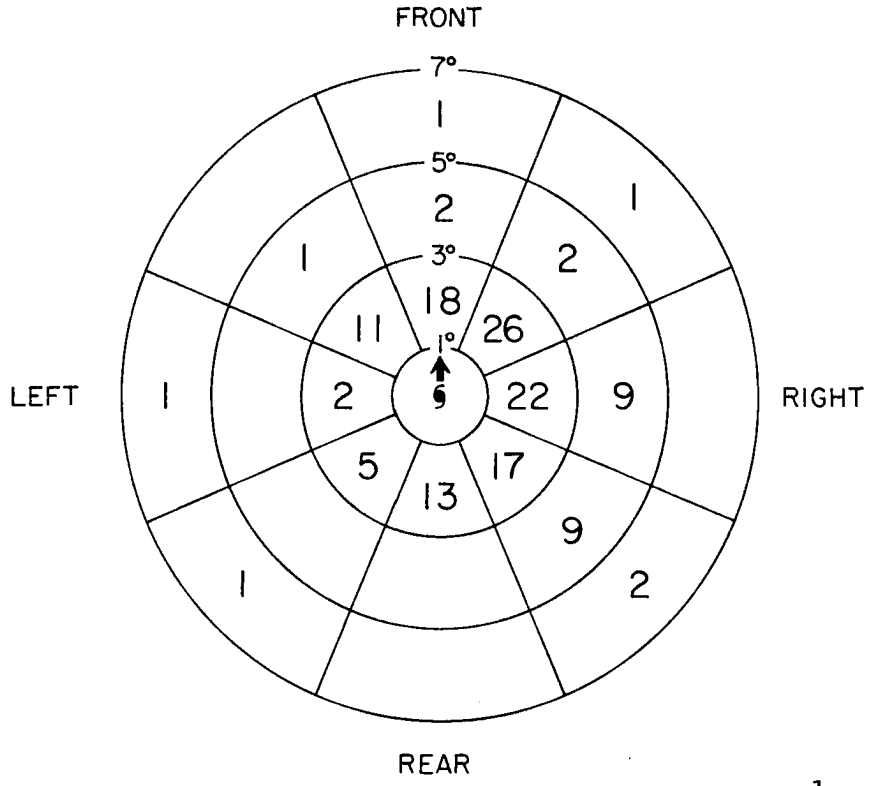

Fig. 41. Percent frequency of 850 mb wind speeds of 20 m s^{-1} or more (approximately 15 m s^{-1} at the surface) around small tropical storms in the Atlantic.

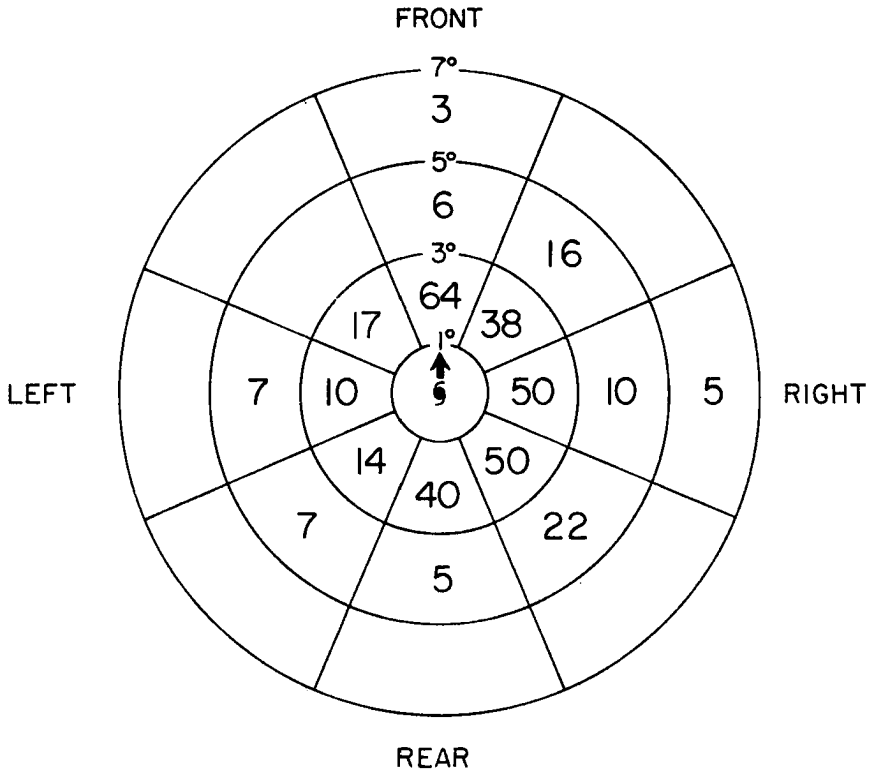

Fig. 42. Same as Fig. 41 except for large tropical storms.

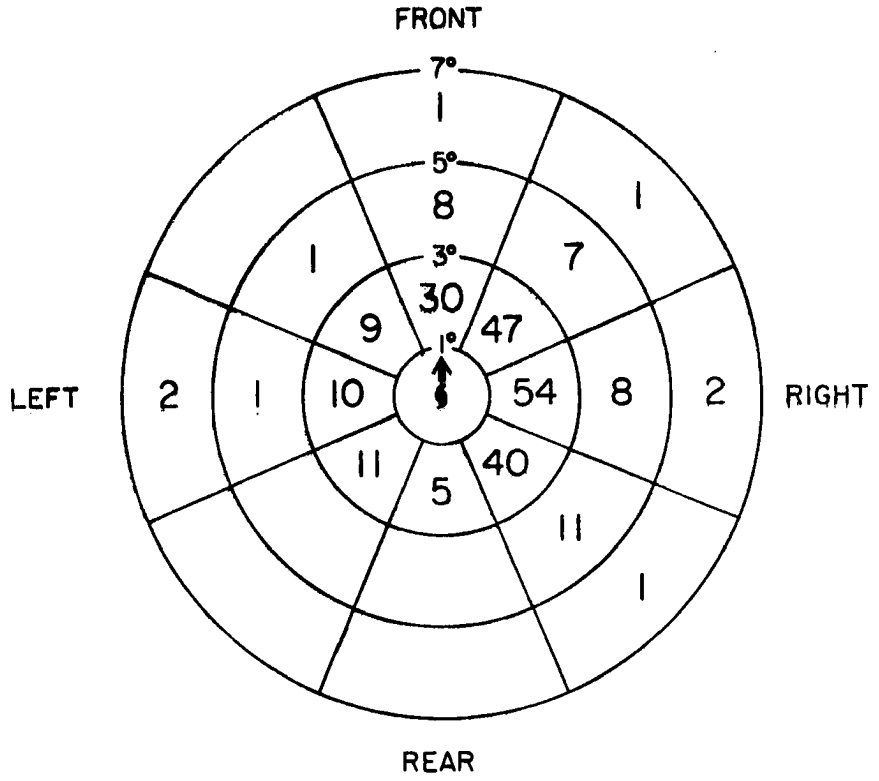

Fig. 43. Same as Fig. 41 except for small hurricanes.

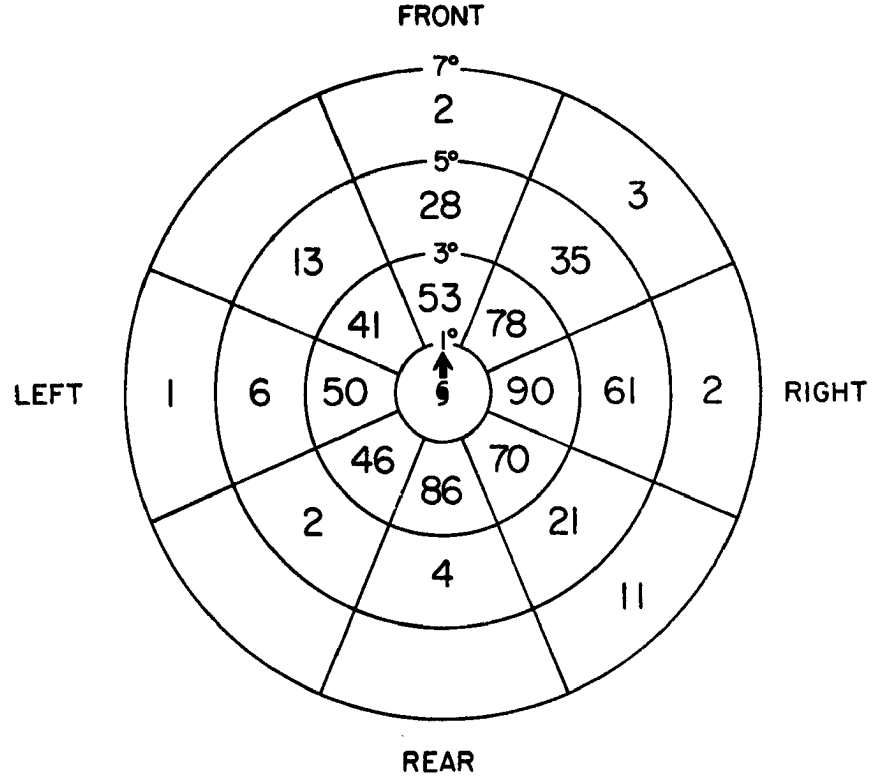

Fig. 44. Same as Fig. 41 except for large hurricanes north of 25° latitude.

5. MAINTENANCE OF LARGE AND SMALL CYCLONES AND ANGULAR MOMENTUM CONSIDERATIONS

5.1 Introduction

In the previous two chapters it has been demonstrated that tropical cyclones exhibit a range of sizes as well as maximum winds, and that different sizes of cyclones tend to occur during particular times of year and in particular locations. Significant structural differences in both wind and mass fields are also apparent - large cyclones logically perturb the basic state of the atmosphere over a larger area than do smaller ones. This chapter discusses the implications of these climatological and structural findings and attempts to provide a physical explanation for the observed characteristics of tropical cyclone size.

5.2 A Discussion of Angular Momentum in Tropical Cyclones

A powerful constraint on the tropical cyclone is the conservation of angular momentum. The angular momentum about the cyclone center is given by

$$\begin{aligned} AAM &= EAM + RAM \\ &= 1/2\ f_o r^2 + rv \end{aligned} \tag{4}$$

where r is radius from the center, f_o is the Coriolis parameter at the latitude of the cyclone center, and v is the tangential wind. The absolute angular momentum (AAM) is the sum of earth angular momentum (EAM) and relative angular momentum (RAM). The tropical cyclone, like

any synoptic storm, is a concentration of cyclonic RAM which must be accumulated and maintained in order for the storm to develop and persist. This concentration is brought about by a circulation which imports angular momentum. Pfeffer (1958), and Holland (1982) have studied the angular momentum fluxes of tropical cyclones and have found that the mean transverse circulation dominates within 400 km of the center. Net inflow occurs in the low and middle troposphere where the tangential wind is strong and cyclonic (high RAM), and net outflow occurs in the upper troposphere, with low RAM. The result is a net import of cyclonic RAM into the cyclone. At radii beyond 400 km, the momentum transports are increasingly the result of horizontal eddy fluxes, particularly in the upper troposphere where large asymmetries are often observed (Black and Anthes, 1971; Lee, 1982).

For the tropical cyclone to remain in steady state, it is necessary that the angular momentum flux into the cyclone offset the surface losses. If the cyclone is also moving poleward (as is usually the case), greater imports of RAM are required to account for the conversion of RAM to EAM (Coriolis torque). Observations show the latter requirement to be several times larger than the former outside the high-energy core of the cyclone (Holland, 1982).

An increase in momentum influx beyond the transports needed to balance friction and EAM changes will increase the RAM of the cyclone. One result would be an increase in lower-tropospheric surface wind and hence surface stress. In time, the increase in surface losses of RAM would equal the increased transports and the cyclone would again approach steady state. What is not immediately clear is how the increase in RAM will be distributed - it could go to increase the

maximum winds (intensification), the average wind speed in the vortex (strength), or the extent of the circulation (growth). In the next section it will be demonstrated that the high-energy core is relatively unimportant to the total angular momentum of the tropical cyclone, while the winds at greater radii are crucial. It is therefore hypothesized that an increased convergence of angular momentum into a tropical cyclone is directly associated with growth and strengthening, but not necessarily with cyclone intensification.

5.3 Observed Angular Momentum Associated with Large and Small Tropical Cyclones

Using the rawinsonde composites described in Chapter 4, the values of relative angular momentum, earth angular momentum, absolute angular momentum, and loss of angular momentum due to surface stress were calculated for 1° latitude radial belts from 2° to 6° and 2° belts from 6° to 14°, from 950 mb to 100 mb.

Because few rawinsonde observations exist inside 2° radius, it was necessary to obtain an approximation to the wind field. It is assumed that the vertically integrated wind field can be approximated by a modified Rankine vortex (Hughes, 1952) of the form

$$v = \begin{cases} v_o\left(\frac{v_o}{V_{max}}\right)^{-1-\frac{1}{x}\frac{r}{r_o}} & 0 \leq r \leq r_{max} \\ v_o\left(\frac{r_o}{r}\right)^{x} & r_{max} \leq r \end{cases} \qquad (5)$$

where

V = tangential wind,

V_o = tangential wind at specified radius r_o,

V_{max} = maximum wind in the vortex,

x = empirical vortex parameter, usually in the range 0.4 to 0.6. It is here set equal to 0.5,

r = radius,

r_o = radius of v_o, here taken to be 2^o latitude or 222 km, and

r_{max} = radius of maximum winds.

Such a profile has been demonstrated to fit surface winds with reasonable accuracy (Riehl and Malkus, 1960) with value of x = 0.5. Shea and Gray (1973) indicate that the value of x in the upper troposphere is closer to 0.75. However, Shea and Gray (1973) also shows that the shape of the tangential wind profile in the high-energy area near the center changes little up to 500 mb, so for this calculation a value of 0.5 will be used.

This profile is used to estimate the radial dependence of the vertically averaged wind inside 2^o radius, using the following steps:

1) Estimate V_{max} using the average maximum winds of the cyclones for which the composite was made.
2) Subtract the mean cyclone speed of motion from the maximum wind to obtain an estimate of the azimuthal average maximum wind.
3) Estimate the surface V_o for r_o at 2^o latitude radius using 75% of the 850 mb composite tangential wind at 2^o.
4) Solve Eq. 5 for r_{max}, using x = 0.5.

5) Use r_{max} obtained in Eq. 4 and assume that r_{max} is constant with height (Shea and Gray, 1973) to obtain vertically averaged r_{max}.

6) Calculate vertically integrated v_o from composite tangential winds at 2^o latitude radius.

7) Use v_o and r_{max} to solve Eq. 5 for estimated vertically averaged V_{max}.

This fitted vortex can be multiplied by r and integrated exactly to yield an estimate of the RAM from the center of the cyclone to 2^o latitude radius. Although the assumed profile shape and estimated r_{mx} for the tropospheric mean vortex are subject to error, an examination of Figs. 45 and 46 show the angular momentum of the $0-2^o$ region to be small when compared with that of the rest of the circulation.

The $0-4^o$ momentum is related to both cyclone size and intensity. The Pacific typhoons have more momentum than Pacific tropical storms, but within each intensity class the momentum content increases monotonically with size. The Atlantic is less consistent, as the large tropical storm has more momentum than the small hurricane, but the dual influence of size and intensity is still apparent. The large hurricane south of 25N is a bit unusual - observations of its relatively low tangential winds at 2^o and strong climatological maximum wind of 45 m s^{-1} (highest of the Atlantic sets) place it as a relatively 'tight' intensifying vortex within a large circulation envelope.

Figure 46 shows the integrated momentum from the center to 8^o. Here, the effect of the assumed Rankine profile from $0-2^o$ (shown in

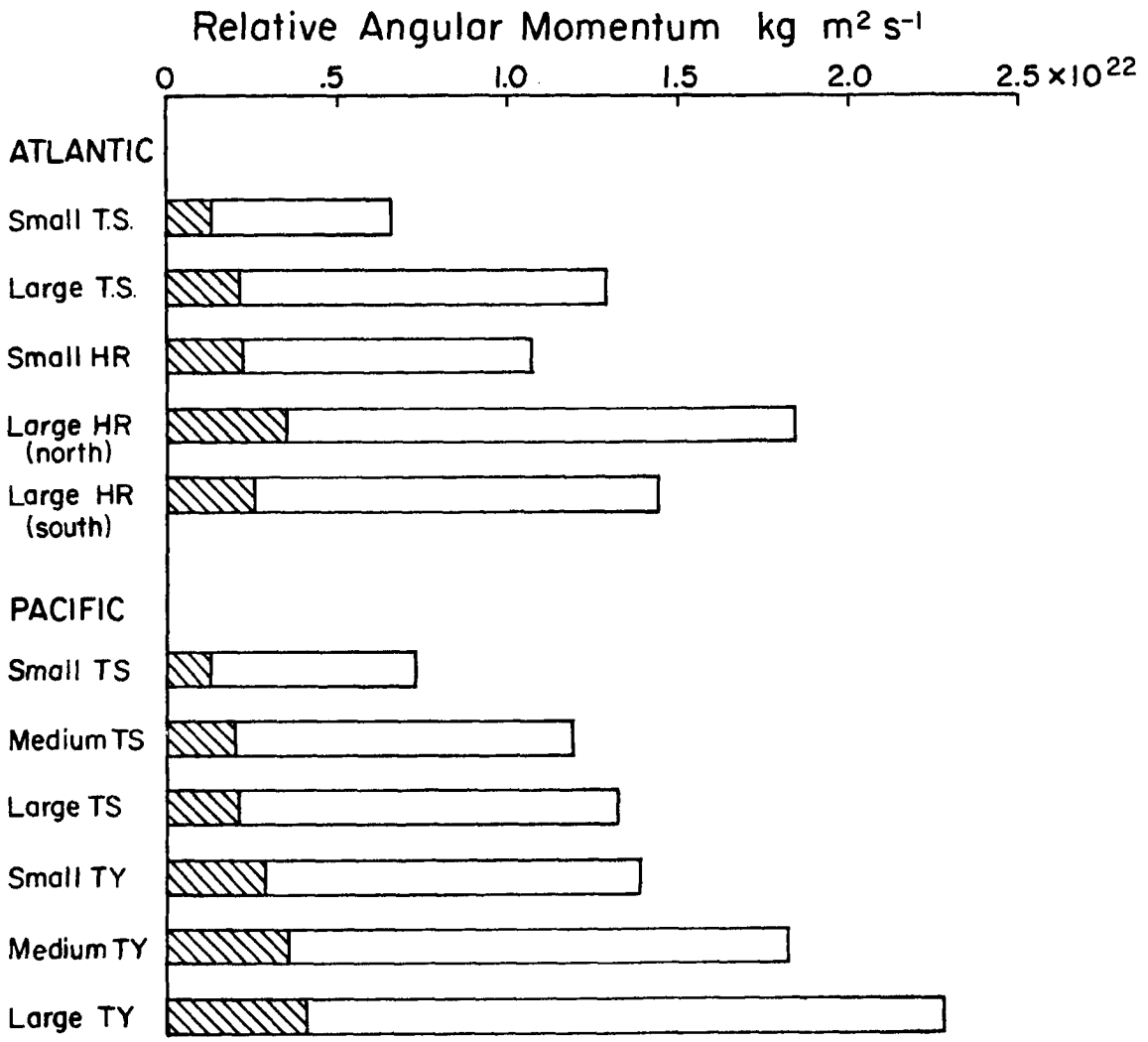

Fig. 45. Integrated relative angular momentum (RAM) from 0^{o}–4^{o} latitude radius and 950 mb to 100 mb for Atlantic and Pacific tropical cyclone composites. The shaded area is the RAM estimated for the 0^{o}–2^{o} region using the fitted modified Rankine vortex approximation described in the text.

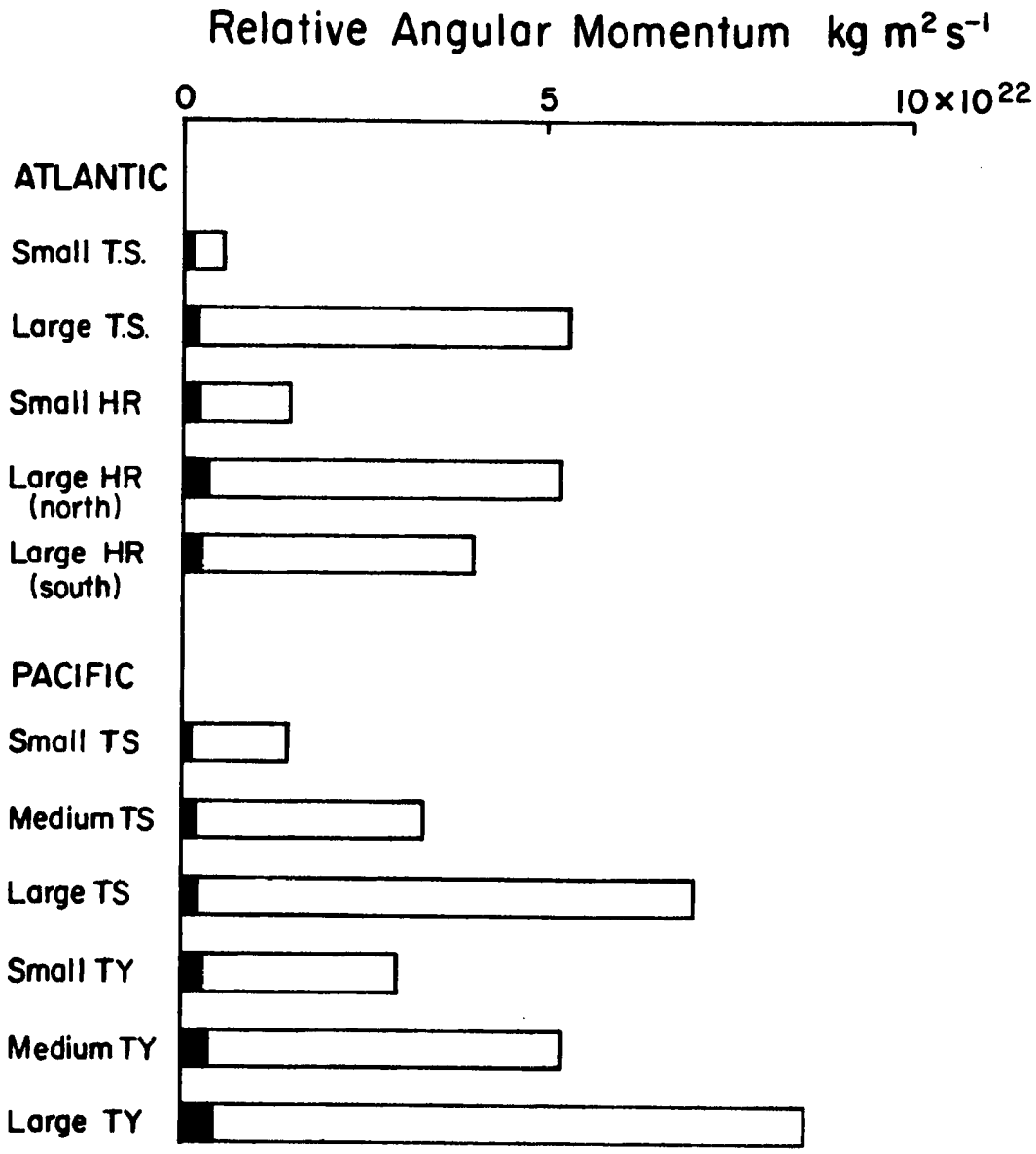

Fig. 46. Same as Fig. 45 except from 0°–8° radius. Shaded area is again the estimated RAM from 0°–2° latitude radius.

black) is negligible, and size is clearly dominant in determining momentum amount. The large tropical storms contain more momentum than all but the large hurricanes and typhoons, and only within a given size class do intense systems necessarily possess more momentum than weaker ones.

Figure 47 shows surface losses of angular momentum, obtained by numerically integrating

$$F = \int_{o}^{2\pi} \int_{0^{o}lat}^{8^{o}lat} \rho r C_D |v_{sfc}| \, v_{sfc} \, r \, dr \, d\theta \qquad (7)$$

where $C_D = 7.5 \times 10^{-4} + 6.7 \times 10^{-5} |v_{sfc}|$ (v_{sfc} in m s^{-1}) (Garratt, 1977; Holland, 1982) using 75% of the 850 mb composite winds as an estimate of surface winds from 2^{o} to 8^{o} radius, and using the fitted Rankine vortex described earlier to estimate the surface winds from 2^{o} radius to the center. Surface stress follows a trend similar to that of RAM - a function of intensity and size at $0-4^{o}$, and more nearly a function of size alone at $0-8^{o}$. Even at 4^{o}, the effects of size are plain - the larger systems are experiencing more surface stress than their smaller counterparts of equal intensity.

5.4 Implications of Angular Momentum Constraints for Cyclone Size and Growth

As discussed in the previous section, large tropical cyclones are observed to have more angular momentum than small ones and, over areas of 4^{o} radius and beyond, size is a more important factor than intensity in determining total cyclone RAM. Surface stresses also follow the same trend - over areas of 8^{o} radius, size is an important control. Several implications arise from these observations.

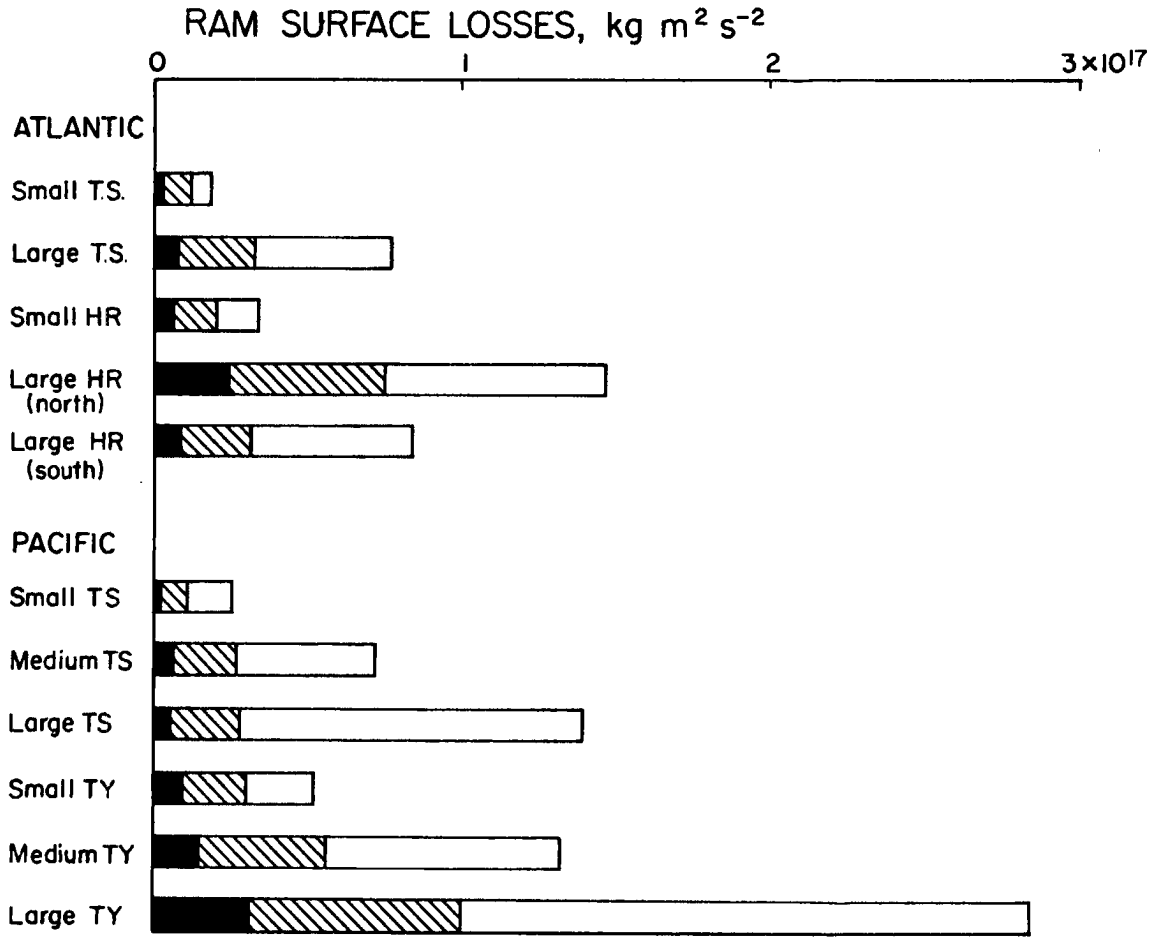

Fig. 47. Integrated surface sink of cyclone RAM from 0^{o}–8^{o} latitude radius fo Atlantic and Pacific tropical cyclone composites. The black area corresponds to surface losses in the area within 2^{o} latitude radius of the center, the hatched area from 2^{o} to 4^{o}, and the remainder from 4^{o} to 8^{o}.

The most obvious implication is that the momentum transports into a large cyclone must be greater than those into a small cyclone, just to maintain it in steady state. The ratio involved is quite large; as can be seen in Fig. 45 the large typhoon is subject to over five times as much surface stress as a small one. The transports required for a growing, moving storm must be larger still. Suppose that a small hurricane were to increase its ROCI by 2^{o} in 36 h, becoming a medium hurricane, while moving northward from 20^{o}N to 22.5^{o}N (an average speed of 2.1 m s^{-1}), and intensifying and strengthening such that the average wind inside 2^{o} latitude (hence the RAM also) were to increase to 1.5 times the 'small hurricane' estimate. The magnitude of the angular momentum transports required are shown in Table 6.

TABLE 6

Angular momentum transports across 8^{o} radius required by a growing, intensifying cyclone.

PROCESSES	IMPORT TO CYCLONE		
	kg $m^{2}s^{-2}$	m $s^{-1}d^{-1}$*	Percent
GROWTH	2.86×10^{17}	1.9	49.5
POLEWARD MOTION	1.94×10^{17}	1.3	33.5
SURFACE STRESS	$.90 \times 10^{17}$	0.6	15.5
INTENSIFICATION AND STRENGTHENING	$.08 \times 10^{17}$	0.1	1.5

*Angular momentum transport expressed as an average increase in tangential wind.

The requirement for growth was described earlier - the tangential wind is increasing at all radii. The 'motion' requirement arises because the system is moving poleward to higher values of the Coriolis parameter and the associated EAM is rising. Under conservation of angular momentum, this too must be accounted for, either by an

equivalent decrease in RAM (which we have specified does not happen) or by transports. Note that the requirement to offset surface losses is smaller than the first two, but of the same order, but the requirement for intensification is negligible.

What happens in nature, of course, is that the environment supplies a quantity of angular momentum and the cyclone responds, rather than the cyclone issuing 'requirements' as in the simple example presented above. A portion of the momentum goes to offset EAM changes as the cyclone moves in response to its environmental flow, and the remainder goes to spin up the wind field.

Growth of a tropical cyclone is hypothesized to result from increasing fluxes of angular momentum at large radii around the vortex. Holland (1982) has derived an equation for the tendency of relative angular momentum in Lagrangian (following the cyclone) coordinates and evaluated the terms using rawinsonde composite data. At large radii, the momentum budget is controlled mainly by three effects: 1) the meridional motion torque, 2) the eddy Coriolis torque and 3) the horizontal eddy RAM flux.

The meridional motion torque arises from the changing value of f with latitude, as described previously. Poleward-moving cyclones experience an anticyclonic torque. The eddy Coriolis torque arises from the relative motion of the environmental flow and the cyclone. If air is flowing through the cyclone from pole to equator, it has a higher value of f when entering than when leaving, and the cyclone experiences a cyclonic torque. Note that the meridional motion and eddy Coriolis torques work similarly, though they often oppose each other, as cyclones usually move poleward faster than the environmental flow (Chan and Gray,

1982). The horizontal eddy RAM flux arises when inflow (outflow) in Lagrangian coordinates (cyclone motion vector subtracted from the winds) coincides with maximum cyclonic (anticyclonic) circulation.

With a growing cyclone we would expect more cyclonic values of these effects. A paradox is that growth is associated with recurvature and poleward motion - an increased anticyclonic motion torque. This is apparently offset by the other effects, however. Figure 48 shows two characteristic lower-tropospheric flows - one associated with a small cyclone and the other with a large or growing one. The presence of an anticyclone (often of polar origin) to the northwest of the growing cyclone results in an increased eddy Coriolis torque in the lower troposphere, and likely an increased eddy RAM flux as well. Because the anticyclone is of polar origin, the meridional flow to the west of the cyclone is vertically sheared with southerlies overlying northerlies. The mean tropospheric wind is still southerly, so the cyclone moves toward the north despite the opposing flow in the lowest levels.

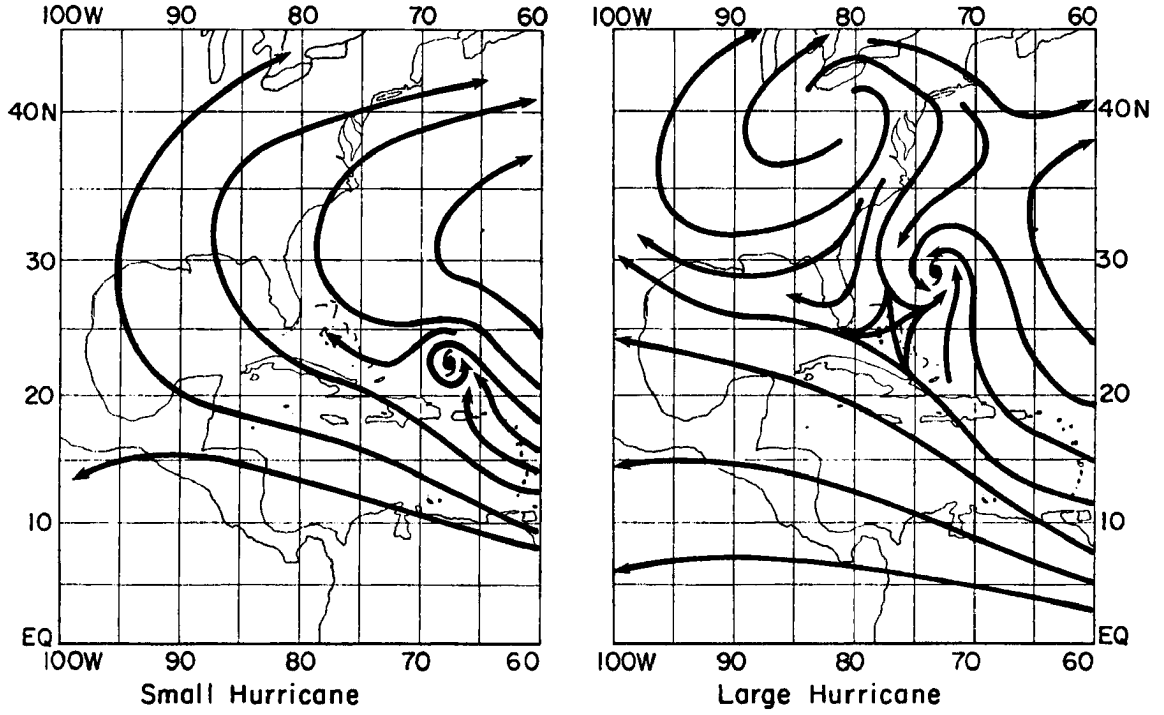

Fig. 48. Examples of environmental lower-tropospheric flows associated with a small cyclone (left) and a large or growing cyclone (right).

6. SUMMARY AND CONCLUSIONS

This paper introduces the relatively unexplored topic of tropical cyclone size. A specification of the structure of a hurricane vortex is presented in terms of three parameters: intensity, size and strength. Size is estimated using the radius of outer closed isobar and a climatology of tropical cyclone size in the northwest Pacific and north Atlantic basins is presented. It is shown that Pacific cyclones are significantly larger, and that seasonal and geographical variability in tropical cyclone size occurs in both basins.

A first look at the structure of large and small tropical cyclones is obtained by compositing rawinsonde observations. Comparisons between large and small cyclones and intense and weak cyclones show the importance of size differences - large systems have lower-tropospheric winds at radii of 4^{o}-6^{o} latitude almost double those of small systems. The area involved in these wind differences is quite large. The effects of variations in intensity are confined to a much smaller area near the cyclone center.

Some of the dynamical implications of these structural differences are examined by computing the angular momentum and surface stresses associated with composite cyclones. When averaged over an area of 6^{o} latitude radius or more, angular momentum and surface losses are related more to size than intensity. An estimate of the horizontal flux of angular momentum required to produce observed rates of cyclone growth

shows it to be several times larger than the flux needed to replace surface losses. Large cyclones occur as a result of formation in a highly cyclonic environment such as a monsoon trough, or by growth. Growth is hypothesized to result from enhanced momentum fluxes into the cyclone, most often as it moves poleward between a subtropical anticyclone and a polar outbreak anticyclone.

Some specific findings of this paper are:

1) The definition of cyclone size based on the radius of outer closed isobar is a physically meaningful one, and the difference in lower tropospheric winds between large and small cyclones is statistically significant.
2) Pacific cyclones are significantly larger than Atlantic cyclones.
3) Large cyclone frequency in both basins reaches a minimum in midsummer (July or August) and a maximum in October.
4) Large cyclones tend to occur in the vicinity of the monsoon trough (Pacific) and in the subtropics in autumn (Atlantic and Pacific).
5) Differences in tangential winds between tropical cyclones of different intensities are mainly confined to radii inside 2^{o}.
6) Absolute angular momentum and surface losses of angular momentum are related more strongly to size than intensity when integrated over radii of 6^{o} or more.
7) Characteristic areas of large cyclone occurrence in the subtropics can be qualitatively explained by increased horizontal fluxes of angular momentum associated with cold surges impinging on the cyclones from the northwest.

Much additional work remains to be done, as tropical cyclone growth, motion and intensification are coupled by means of vortex-environment interactions. Of particular interest is the relationship between cyclone size, strength and intensity - growth seems explainable as a direct result of increased angular momentum fluxes into the cyclone, while strength and intensity changes are controlled by other factors as well. A later research paper will attempt to address intensification directly. Additional work planned on tropical cyclone size will be efforts to develop information of operational use, such as a pressure-wind relationship including the effects of size, detailed statistics of the radius of gales around cyclones of different sizes, and a survey of the effect of cyclone size on hurricane surge and rainfall. Efforts will also be made to determine whether the increased momentum fluxes can be consistently related to growth as has been hypothesized, and in exactly what ways the increased fluxes occur.

ACKNOWLEDGEMENTS

This work represents the culmination of the labors, support and hopes of many. I am especially indebted to my advisor, Professor William M. Gray, for the continued opportunity and encouragement to work on this and related topics. Thanks go to: Professor Gray and members of his project, Greg Holland, Johnny Chan, Jianmin Xu, Clifford Matsumoto, and Cheng-Shang Lee for many fine discussions and words of advice; Janet Gray for keypunching the Atlantic size data set; Norine Haley for data reduction and plotting; Cindy Schrandt and Susan Cavender for typing; Edwin Buzzell and many former students for rawinsonde data sets used in compositing; and to Barbara Brumit for typing and keeping the whole show going.

This work was accomplished while the author was a National Science Foundation Graduate Fellow. Recommendation from the National Hurricane Center was instrumental in the obtaining this fellowship.

This research has been financially supported by NOAA Grant No. NA81RAD00005 and Grant No. NA81RAH00001 and NSF Grant No. ATM-7923591

Above all, thanks to my parents for believing.

REFERENCES

Arakawa, H., 1950: Mame-taifu or midget typhoon. Geophys. Mag., 23, 463-474.

Atkinson, G. D., 1971: Forecaster's guide to tropical meteorology. AWS Tech. Rept. 240, US Air Force.

Atkinson, G. D. and C. R. Holliday, 1977: Tropical cyclone minimum sea level pressure/maximum sustained wind relationship for the western north Pacific. Mon. Wea. Rev., 105, 421-427.

Australian Bureau of Meteorology, 1977: Report on cyclone Tracy, December, 1974. Australian Government Publishing Service, Canberra, 82 pp.

Black, P. G. and R. A. Anthes, 1971: On the asymmetric structure of the tropical cyclone outflow layer. J. Atmos. Sci., 28, 1348-1366.

Brand, S., 1972: Very large and very small typhoons of the western north Pacific Ocean. J. Meteor. Soc. Japan, 50, 332-341.

Chan, J. C. L. and W. M. Gray, 1982: Tropical cyclone motion and surrounding parameter relationships. Submitted to Mon. Wea. Rev.

Chan, J. C. L., W. M. Gray and S. Q. Kidder, 1980: Forecasting tropical cyclone turning motion from surrounding wind and temperature fields. Mon. Wea. Rev., 108, 778-792.

Ding, Y. H. and E. R. Reiter, 1980: A preliminary study of the variability in the frequency of typhoon formation over the west Pacific Ocean. Environmental Research Paper 22, Colo. State Univ., Fort Collins, CO, 21 pp.

Dunn, G. E. and B. I. Miller, 1960: Atlantic Hurricanes. Louisiana State Univ. Press, Baton Rouge, LA, 326 pp.

Dunnavan, G. M. and J. W. Diercks, 1980: An analysis of super typhoon Tip (October 1979). Mon. Wea. Rev., 108, 1915-1923.

Dvorak, V. F., 1975: Tropical cyclone intensity analysis and forecasting from satellie imagery. Mon. Wea. Rev., 103, 420-430.

Frank, W. M., 1977: The structure and energetics of the tropical cyclone, Part I: Storm structure. Mon. Wea. Rev., 105, 1119-1135.

Frank, W. M. and W. M. Gray, 1980: Radius and frequency of 15 m s^{-1} (30 kt) winds around tropical cyclones. J. Appl. Meteor., 19, 219-223.

REFERENCES (cont'd)

Garratt, J. R., 1977: Review of drag coefficients over oceans and continents. Mon. Wea. Rev., 105, 915-929.

Gray, W. M., 1979: Hurricanes: their formation, structure and likely role in the tropical circulation. Supplement to Meteorology Over the Tropical Oceans. Published by RMS, James Glaisher House, Grenville Place, Bracknell, Berkshire, R6 12 1BX, D. B. Shaw, Ed., 155-218.

Gray, W. M., E. Buzzell, G. Burton and Other Project Personnel, 1982: Tropical cyclone and related meteorological data sets available at CSU and their utilization. Dept. of Atmos. Sci. Paper, Colo. State Univ., Ft. Collins, CO, 186 pp.

George, J. E. and W. M. Gray, 1977: Tropical cyclone recurvature and non-recurvature as related to surrounding wind-height fields. J. Appl. Meteor., 16, 34-42.

Holland, G. J., 1982: Angular momentum transports in tropical cyclones. Accepted for publication by Quart. J. Roy. Meteor. Soc.

Hughes, L. A., 1952: On the low-level wind structure of tropical storms. J. Meteor., 9, 422-428.

Jarvinen, B. R. and E. L. Caso, 1978: A tropical cyclone data tape for the north Atlantic basin, 1886-1977: contents, limitations and uses. NOAA Tech. Memo., NWS NHC-6, 19 pp.

Lee, C. S., 1982: Cumulus momentum transports in tropical cyclones. Dept. of Atmos. Sci. Paper No. 341, Colo. State Univ., Ft. Collins, CO, 78 pp.

Love, G., 1982: The role of the general circulation in western Pacific tropical cyclone genesis. Dept. of Atmos. Sci. Paper No. 340, Colo. State Univ., Ft. Collins, CO, 215 pp.

McBride, J. L. and R. Zehr, 1981: Observational studies of tropical cyclone formation, Part II: Comparison of non-developing versus developing systems. J. Atmos. Sci., 1132-1151.

Mosteller, F. and R. E. K. Rourke, 1973: Sturdy statistics. Addison-Wesley Publishing Co., Reading, MA, 395 pp.

Pfeffer, R. L., 1958: Concerning the mechanics of hurricanes. J. Meteor., 15, 113-120.

Riehl, H., 1979: Climate and weather in the tropics. Academic Press, London, 611 pp.

Riehl, H. and J. S. Malkus, 1960: On the dynamics and energy transformations in steady-state hurricanes. Tellus, 12, 1-20.

REFERENCES (cont'd)

Shea, D. J. and W. M. Gray, 1973: The hurricane's inner core regions, I: Symmetric and asymmetric structure. J. Atmos. Sci., 30, 1544-1564.

Walpole, R. E. and R. H. Myers, 1978: Probability and statistics for engineers and scientists. Macmillan, Collier, New York, 580 pp.

Zipser, E. J., 1964: On the thermal structure of developing tropical cyclones. NHRP Report 67, National Hurricane Research Project, Miami, FL, 23 pp.

APPENDIX

The mean azimuthal mean tangential winds for the composite tropical cyclones described in Chapter 4 are shown below.

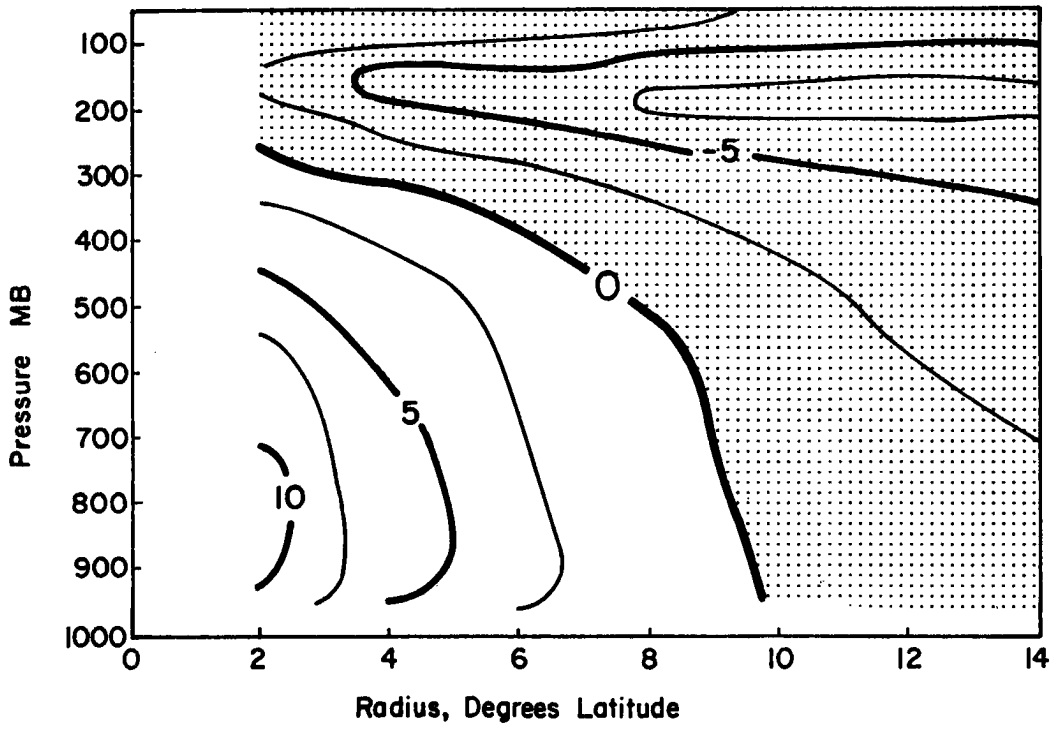

Fig. 49. Azimuthal mean tangential wind for the composite Atlantic small/medium tropical storm.

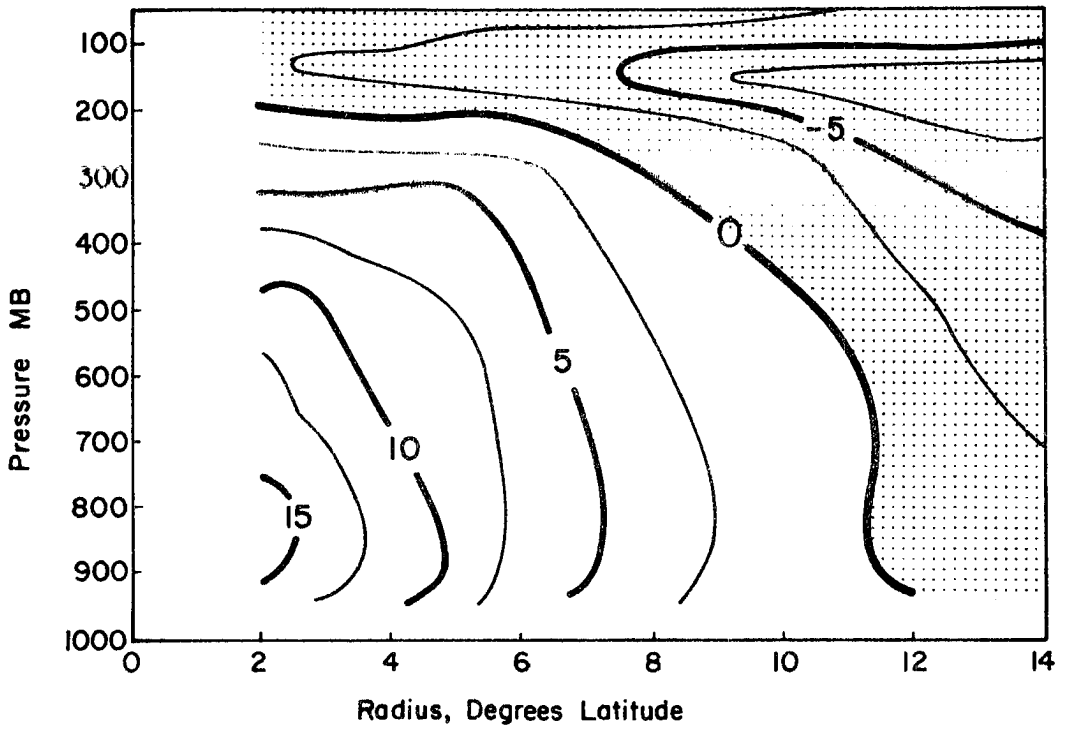

Fig. 50. Same as Fig. 49 except for the Atlantic large tropical storm.

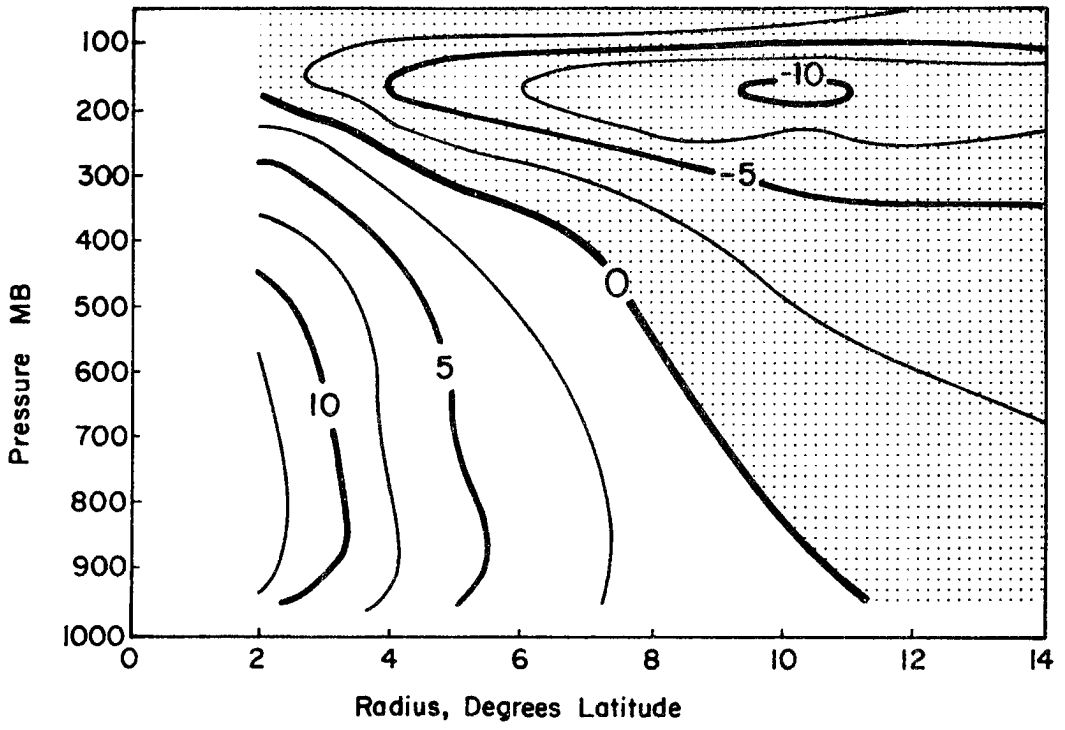

Fig. 51. Same as Fig. 49 except for the Atlantic small/medium hurricane.

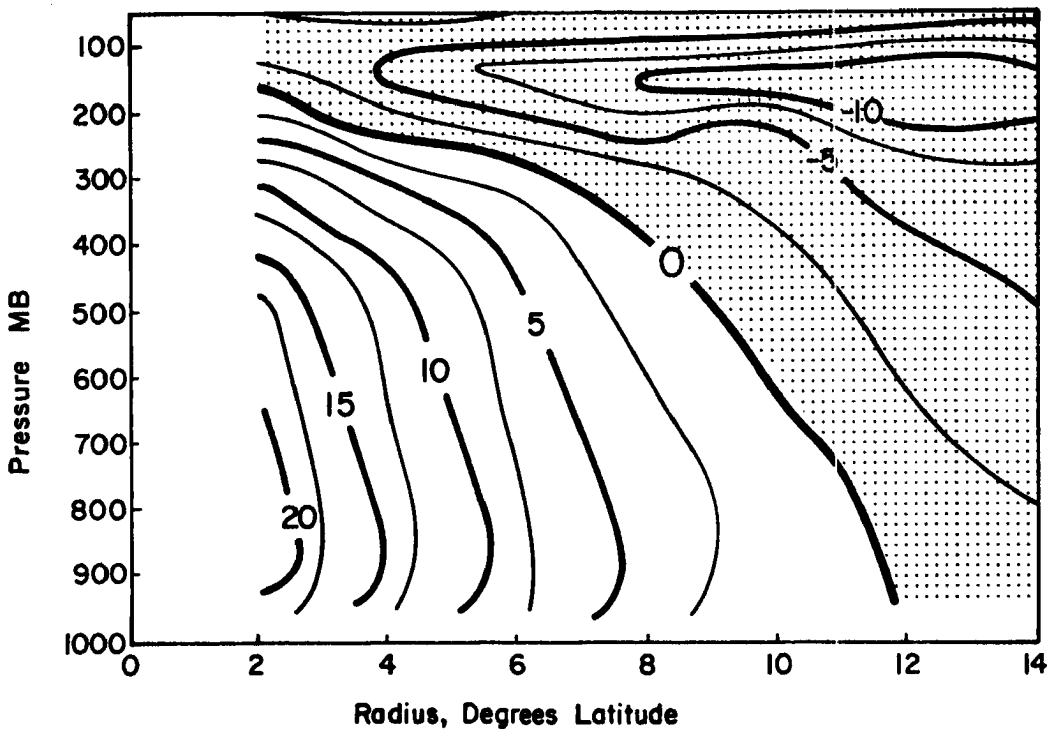

Fig. 52. Same as Fig. 49 except for the Atlantic large hurricane north of 25N.

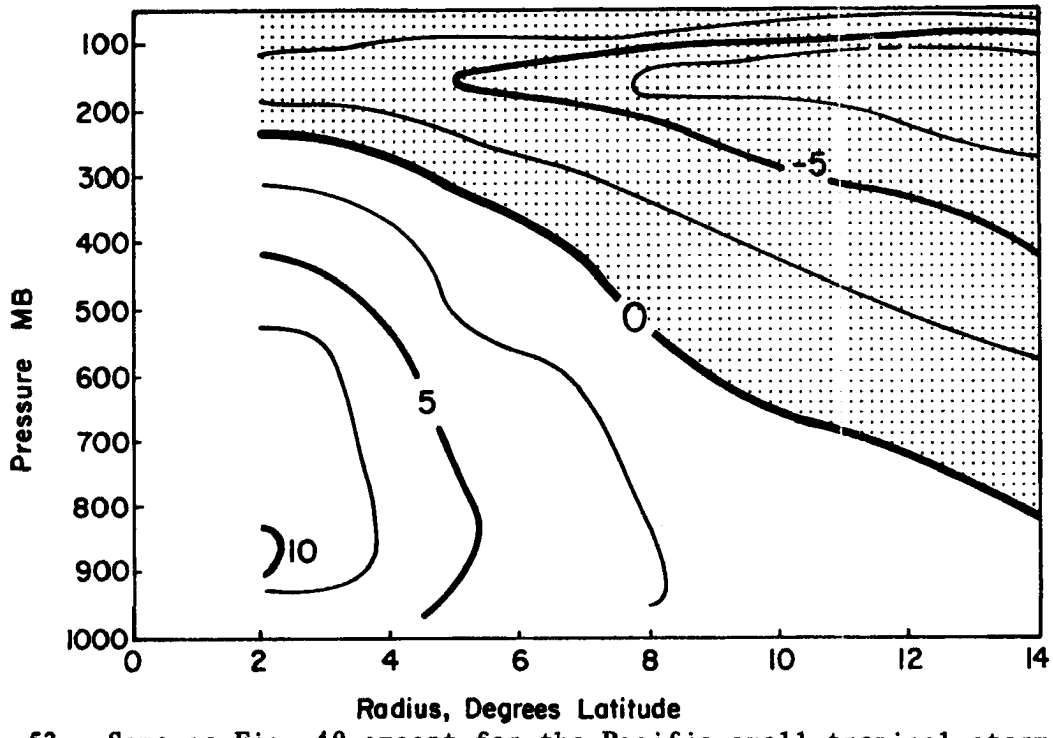

Fig. 53. Same as Fig. 49 except for the Pacific small tropical storm.

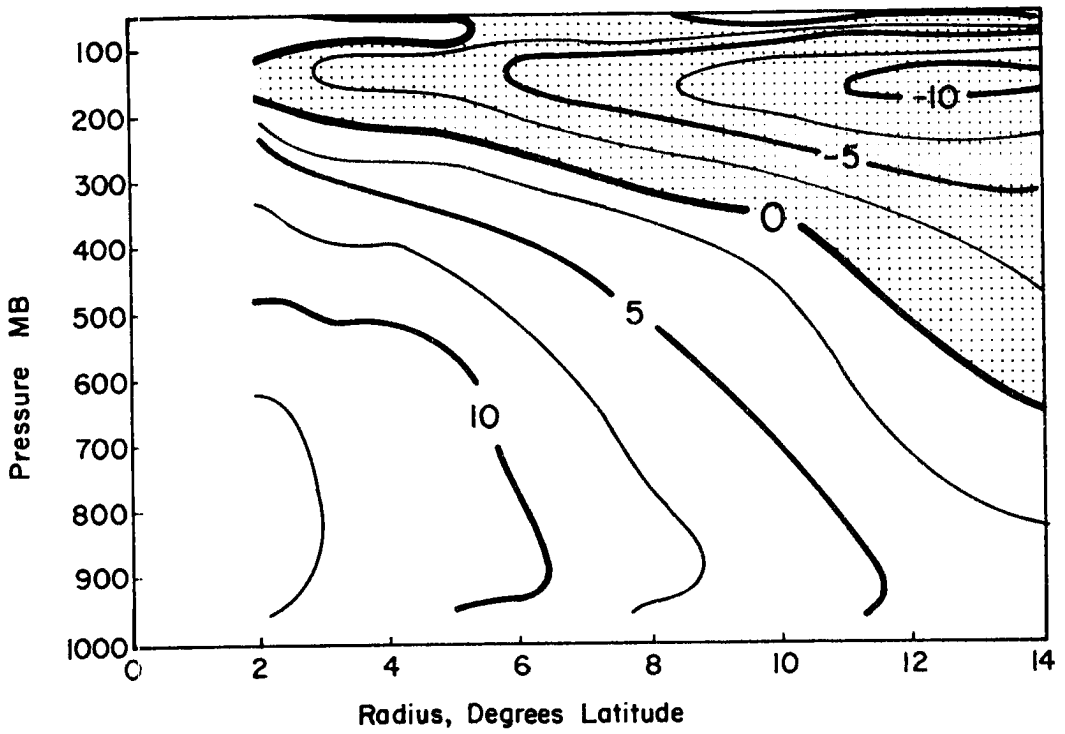

Fig. 54. Same as Fig. 49 except for the Pacific large tropical storm.

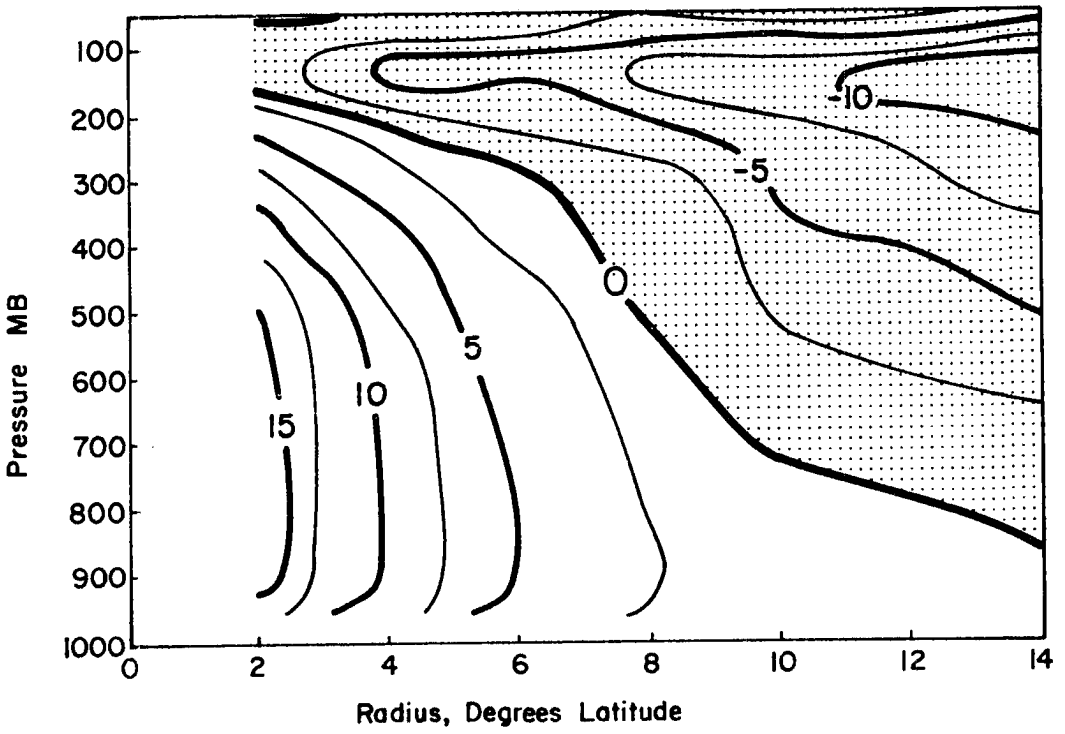

Fig. 55. Same as Fig. 49 except for the Pacific small typhoon.

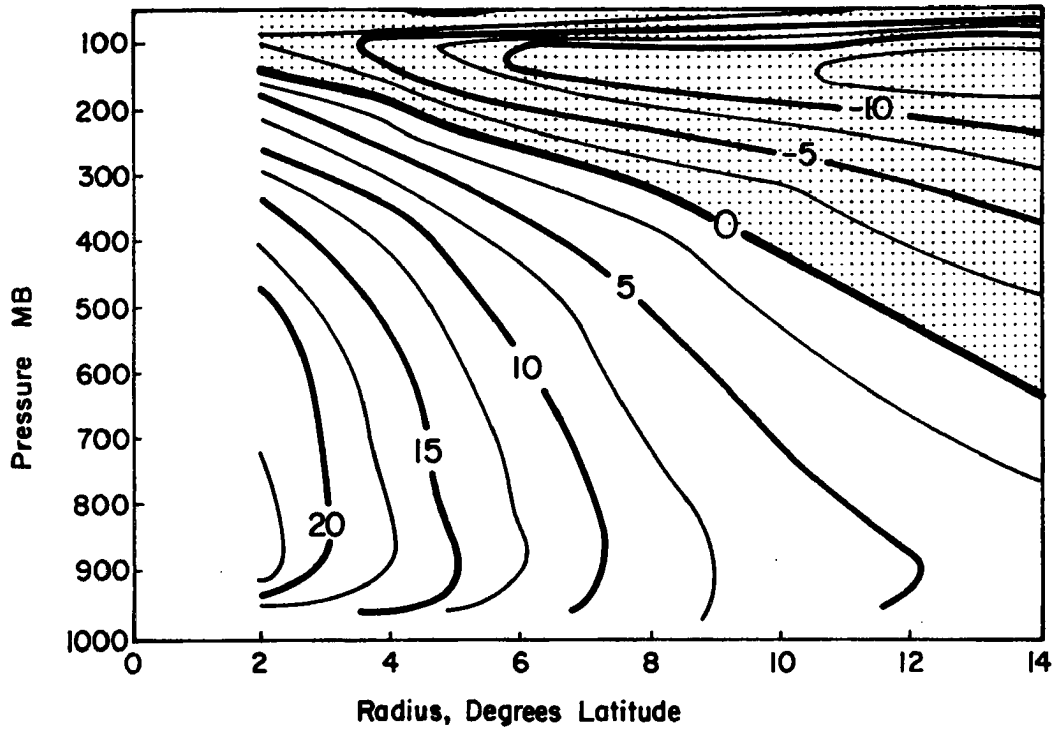

Fig. 56. Same as Fig. 49 except for the Pacific large typhoon.

W. M. GRAY'S FEDERALLY SUPPORTED RESEARCH PROJECT REPORTS SINCE 1967

CSU Dept. of Atmos. Sci. Report No.	Report Title, Author, Date, Agency Support
104	The Mutual Variation of Wind, Shear and Baroclinicity in the Cumulus Convective Atmosphere of the Hurricane (69 pp.). W. M. Gray. February 1967. NSF Support.
114	Global View of the Origin of Tropical Disturbances and Storms (105 pp.). W. M. Gray. October 1967. NSF Support.
116	A Statistical Study of the Frictional Wind Veering in the Planetary Boundary Layer (57 pp.). B. Mendenhall. December 1967. NSF and ESSA Support.
124	Investigation of the Importance of Cumulus Convection and Ventilation in Early Tropical Storm Development (88 pp.). R. Lopez. June 1968. ESSA Satellite Lab. Support.
Unnumbered	Role of Angular Momentum Transports in Tropical Storm Dissipation over Tropical Oceans (46 pp.). R. F. Wachtmann. December 1968. NSF and ESSA Support.
Unnumbered	Monthly Climatological Wind Fields Associated with Tropical Storm Genesis in the West Indies (34 pp.). J. W. Sartor. December 1968. NSF Support.
140	Characteristics of the Tornado Environment as Deduced from Proximity Soundings (55 pp.). T. G. Wills. June 1969. NOAA and NSF Support.
161	Statistical Analysis of Trade Wind Cloud Clusters in the Western North Pacific (80 pp.). K. Williams. June 1970. ESSA Satellite Lab. Support.
---	A Climatology of Tropical Cyclones and Disturbances of the Western Pacific with a Suggested Theory for Their Genesis/ Maintenance (225 pp.). W. M. Gray. NAVWEARSCHFAC Tech. Paper No. 19-70. November 1970. (Available from US Navy, Monterey, CA). US Navy Support.
179	A diagnostic Study of the Planetary Boundary Layer over the Oceans (95 pp.). W. M. Gray. February 1972. Navy and NSF Support.
182	The Structure and Dynamics of the Hurricane's Inner Core Area (105 pp.). D. J. Shea. April 1972. NOAA and NSF Support.

CSU Dept. of Atmos. Sci. Report No.	Report Title, Author, Date, Agency Support
188	Cumulus Convection and Larger-scale Circulations, Part I: A Parametric Model of Cumulus Convection (100 pp.). R. E. Lopez. June 1972. NSF Support.
189	Cumulus Convection and Larger-scale Circulations, Part II: Cumulus and Meso-scale Interactions (63 pp.). R. E. Lopez. June 1972. NSF Support.
190	Cumulus Convection and Larger-scale Circulations, Part III: Broadscale and Meso-scale Considerations (80 pp.). W. M. Gray. July 1972. NOAA-NESS Support.
195	Characteristics of Carbon Black Dust as a Tropospheric Heat Source for Weather Modification (55 pp.). W. M. Frank. January 1973. NSF Support.
196	Feasibility of Beneficial Hurricane Modification by Carbon Black Seeding (130 pp.). W. M. Gray. April 1973. NOAA Support.
199	Variability of Planetary Boundary Layer Winds (157 pp.). L. R. Hoxit. May 1973. NSF Support.
200	Hurricane Spawned Tornadoes (57 pp.). D. J. Novlan. May 1973. NOAA and NSF Support.
212	A Study of Tornado Proximity Data and an Observationally Derived Model of Tornado Genesis (101 pp.). R. Maddox. November 1973. NOAA Support.
219	Analysis of Satellite Observed Tropical Cloud Clusters (91 pp.). E. Ruprecht and W. M. Gray. May 1974. NOAA/ NESS Support.
224	Precipitation Characteristics in the Northeast Brazil Dry Region (56 pp.). R. P. L. Ramos. May 1974. NSF Support.
225	Weather Modification through Carbon Dust Absorption of Solar Energy (190 pp.). W. M. Gray, W. M. Frank, M. L. Corrin, and C. A. Stokes. July 1974.
234	Tropical Cyclone Genesis (121 pp.). W. M. Gray. March 1975. NSF Support.

CSU Dept. of Atmos. Sci. Report No.	Report Title, Author, Date, Agency Support
---	Tropical Cyclone Genesis in the Western North Pacific (66 pp.). W. M. Gray. March 1975. US Navy Environmental Prediction Research Facility Report. Tech. Paper No. 16-75. (Available from the US Navy, Monterey, CA). Navy Support.
241	Tropical Cyclone Motion and Surrounding Parameter Relationships (105 pp.). J. E. George. December 1975. NOAA Support.
243	Diurnal Variation of Oceanic Deep Cumulus Convection. Paper I: Observational Evidence, Paper II: Physical Hypothesis (106 pp.). R. W. Jacobson, Jr. and W. M. Gray. February 1976. NOAA-NESS Support.
257	Data Summary of NOAA's Hurricanes Inner-Core Radial Leg Flight Penetrations 1957-1967, and 1969 (245 pp.). W. M. Gray and D. J. Shea. October 1976. NSF and NOAA Support.
258	The Structure and Energetics of the Tropical Cyclone (180 pp.). W. M. Frank. October 1976. NOAA-NHEML, NOAA-NESS and NSF Support.
259	Typhoon Genesis and Pre-typhoon Cloud Clusters (79 pp.). R. M. Zehr. November 1976. NSF Support.
Unnumbered	Severe Thunderstorm Wind Gusts (81 pp.). G. W. Walters. December 1976. NSF Support.
262	Diurnal Variation of the Tropospheric Energy Budget (141 pp.). G. S. Foltz. November 1976. NSF Support.
274	Comparison of Developing and Non-developing Tropical Disturbances (81 pp.). S. L. Erickson. July 1977. US Army Support.
---	Tropical Cyclone Research by Data Compositing (79 pp.). W. M. Gray and W. M. Frank. July 1977. US Navy Environmental Prediction Research Facility Report. Tech. Paper No. 77-01. (Available from the US Navy, Monterey, CA). Navy Support.
277	Tropical Cyclone Cloud and Intensity Relationships (154 pp.). C. P. Arnold. November 1977. US Army and NHEML Support.
297	Diagnostic Analyses of the GATE A/B-scale Area at Individual Time Periods (102 pp.). W. M. Frank. November 1978. NSF Support.

CSU Dept. of Atmos. Sci. Report No.	Report Title, Author, Date, Agency Support
298	Diurnal Variability in the GATE Region (80 pp.). J. M. Dewart. November 1978. NSF Support.
299	Mass Divergence in Tropical Weather Systems, Paper I: Diurnal Variation; Paper II: Large-scale Controls on Convection (109 pp.). J. L. McBride and W. M. Gray. November 1978. NOAA-NHEML Support.
---	New Results of Tropical Cyclone Research from Observational Analysis (108 pp.). W. M. Gray and W. M. Frank. June 1978. US Navy Environmental Prediction Research Facility Report. Tech. Paper No. 78-01. (Available from the US Navy, Monterey, CA). Navy Support.
305	Convection Induced Temperature Change in GATE (128 pp.). P. G. Grube. February 1979. NSF Support.
308	Observational Analysis of Tropical Cyclone Formation (230 pp.). J. L. McBride. April 1979. NOAA-NHEML, NSF and NEPRF Support.
333	Tropical Cyclone Intensity Change - A Quantitative Forecasting Scheme. K. M. Dropco. May 1981. NOAA Support.
340	The Role of the General Circulation in Tropical Cyclone Genesis (230 pp.). G. Love. April 1982. NSF Support.
341	Cumulus Momentum Transports in Tropical Cyclones (78 pp.). C. S. Lee. May 1982. ONR Support.
343	Tropical Cyclone Movement and Surrounding Flow Relationships (68 pp.). J. C. L. Chan and W. M. Gray. May 1982. ONR Support.
346	Environmental Circulations Associated with Tropical Cyclones Experiencing Fast, Slow and Looping Motions (273 pp.). J. Xu and W. M. Gray. May 1982. ONR Support.
348	Tropical Cyclone Motion: Environmental Interaction Plus a Beta Effect (47 pp.). G. J. Holland. May 1982. ONR Support.
---	Tropical Cyclone and Related Meteorological Data Sets Available at CSU and Their Utilization (186 pp.). W. M. Gray, E. Buzzell, G. Burton and Other Project Personnel. February 1982. NSF, ONR, NOAA, and NEPRF Support.